CEAS Aeronautical Journal (2023) 14:3–28
https://doi.org/10.1007/s13272-022-00627-w

ORIGINAL PAPER

Comparative environmental life cycle assessment and operating cost analysis of long-range hydrogen and biofuel fueled transport aircraft

Kristina Kossarev[1] · **Anna Elena Scholz**[1] · **Mirko Hornung**[1]

Received: 18 August 2022 / Revised: 2 November 2022 / Accepted: 9 November 2022 / Published online: 2 December 2022

Abstract

The aviation industry is currently experiencing a social shift in the attitude towards flying due to the increasing awareness of the impact on climate change. This has led governments and industries to set emissions targets, although their achievement for long-range flights is subject to an ongoing debate. Among promising candidates are hydrogen and sustainable aviation fuels such as biofuel. To provide a meaningful ecological and economic assessment, an environmental life cycle assessment method supplemented by a direct operating cost analysis has been developed and is described in this paper. A wide-body transport aircraft (A330 class) serves as a reference design for developing conceptual aircraft designs with a planned entry-into-service in 2040 powered by liquid hydrogen or drop-in biofuels (based on algae, produced with oil-rich biomass (BtL) or hydrogenated vegetable oil (HVO) processes). Due to the large demand for assumptions, the ecological and economic assessment results have to be interpreted as benchmarks. The results for long-range aircraft show that based on the current fuel and energy production methods both hydrogen and biofuel as aviation fuel are more harmful (have a higher environmental impact) than conventional aircraft. For hydrogen aircraft, an increase in energy consumption of 2.87% leads to an increased environmental impact of 14.8%. Due to the high energy demand for biofuel production, its environmental impact increases by 548% (BtL) and 238% (HVO). Nevertheless, for a future scenario based on electrolysis as a hydrogen production process and on renewable energy to generate electricity, both hydrogen and biofuel-powered aircraft are less harmful when compared to the reference aircraft. The environmental impact reduces by 59.5% (hydrogen), 35.8% (BtL), and 112% (HVO). However, the introduction of the new propellants involves a high direct operating cost penalty of 10.8% for hydrogen and 108% for both biofuels.

Keywords Aircraft design · Hydrogen · Sustainable aviation fuel · Environmental life cycle assessment · Operating costs

List of symbols

A_m	Lateral surface area, m^2
c_p''	Specific heat capacity of steam, J/(gK)
EI	Emission index, g/kg
$EINO_x$	NO_x emission index, g/kg
FA	Fuel-to-air ratio
h_v	Specific enthalpy of vaporization, J/g
$\dot{m}$	Mass flow, g/s
P	Pressure, MPa
$ppmNO_x$	NO_x parts-per-million, 10^{-6}
T	Temperature, K
t	Thickness, m
$\eta_{grav,tank}$	Gravimetric tank efficiency
λ	Thermal conductivity, W/(mK)
ϕ	Equivalence ratio
τ	Combustor residence time, ms
$\dot{Q}$	Heat flow, J/s

Subscripts

3	Engine station three
H_2	Hydrogen
GH_2	Gaseous hydrogen
LH_2	Liquid hydrogen
NO_x	Nitrogen oxides
o	Outside
Insu	Insulation

✉ Kristina Kossarev
kristina.kossarev@tum.de

Anna Elena Scholz
anna.scholz@tum.de

Mirko Hornung
mirko.hornung@tum.de

[1] Technical University of Munich, Boltzmannstr. 15, 85748 Garching, Germany

Abbreviations

A332-K	Long-range kerosene aircraft
A332-H	Long-range hydrogen aircraft
A332-BF	Long-range biofuel aircraft
ADEBO	Aircraft design box
AEA	Association of European Airlines
AHEAD	Advanced hybrid engines for aircraft development
ATA	Air Transport Association of America
BtL	Biomass-to-liquid
CFRP	Carbon fiber reinforced plastics
CtL	Carbon-to-liquid
C3/C4	Configuration 3 or 4
DOC	Direct operating cost
EIS	Entry into service
eLCA	Environmental life cycle assessment
ELCD	European reference life cycle database
EPNdB	Effective perceived noise in decibels
FAR	Federal aviation regulations
FT	Fischer-Tropsch
HEFA	Hydroprocessed esters and fatty acids
HVO	Hydrogenated vegetable oils
ICAO	International Civil Aviation Organization
LEEA	Low emissions effect aircraft
LH_2	Liquid hydrogen
LHV	Lower heating value
MTOM	Maximum take-off mass
NASA	National Aeronautics and Space Administration
OEM	Operating empty mass
PrADO	Preliminary aircraft design and optimization program
SAF	Sustainable aviation fuel
SS	Single score
TLAR	Top level aircraft requirement
TSFC	Thrust specific fuel consumption
TUB	Technical University of Berlin

1 Introduction

The growing awareness of greenhouse gas emissions and the dwindling fossil fuel resources have led the aviation industry to contemplate new propellants and advanced low-carbon propulsion technologies [1]. Hydrogen and sustainable aviation fuels (SAF) such as biofuel are considered promising candidates to attain the given emission targets.

Hydrogen as an energy carrier offers, among others, the advantage of a high climate reduction potential as its direct combustion does not emit CO_2. However, its storage poses a technical challenge due to its low volumetric energy density even in a liquid phase. Numerous previous studies (e.g. [1–6]) demonstrate the technical feasibility of liquid hydrogen (LH_2) as a propellant and present conceptual aircraft designs exploiting different applications (e.g. sub- to supersonic, short- to long-range, etc.). For example, in the CRYOPLANE study of 2000 [1], a detailed system analysis of liquid hydrogen-fueled aircraft was funded by the European Commission in cooperation with Airbus and 34 other partner companies. The main objective was to provide a theoretical basis for the applicability, safety, and environmental compatibility of hydrogen as an aviation fuel for aircraft categories from business jets to very large long-range aircraft. The analysis has shown that hydrogen could be a suitable, climate beneficial, but economical unattractive alternative. Further research would be required due to missing materials or parts and due to the lack of understanding the impact of water emissions. A more recent study emerged from the H2020 Framework Program [6] also deals with the assessment of the potential of hydrogen propulsion to reduce aviation's climate impact. It supports the CRYOPLANE results and adds that a challenging but not impossible hydrogen production scale-up would be required. It is expected that the global hydrogen demand would reach 40 to 130 million tons of LH_2 per annum by 2050 representing 10 to 25% of the global demand considering that maximum 60% of all aircraft switch to LH_2. For the remaining aircraft, SAFs were considered within the H2020 study, which are already used blended in with conventional fuel since 2016 [7]. Various types (such as Fischer-Tropsch (FT) based SAFs) are prosperous future unblended or 100% drop-in fuels allowing a full fossil fuel substitution.

However, existing studies do not provide complete and transparent environmental and economic reviews of the respective configurations. The results presented in the CRYOPLANE study in terms of ecological and economical analysis are focused on short-range aircraft and are limited in publicly available data [1]. Also, Brewer presents a detailed analysis of the hydrogen aircraft technology and its impact on operational aspects on, e.g., airports in his book from 1991 [2]. However, the used method of direct operating costs is not up-to-date, and the environmental consideration does focus only on air pollution at airports and during cruise and not on a complete life cycle assessment. A newer study from Troeltsch et al. investigates a hydrogen-powered long-range aircraft, which also solely assesses in-flight emissions and does not consider the economical analysis [5]. Therefore, to provide a meaningful evaluation in terms of the environmental impact, a full environmental life cycle assessment (eLCA) is necessary. A direct operating cost (DOC) model enables to examine the financial impact of airlines in respect of the prospects of new aviation fuels. Considering the aforementioned shortcomings of previous studies, the

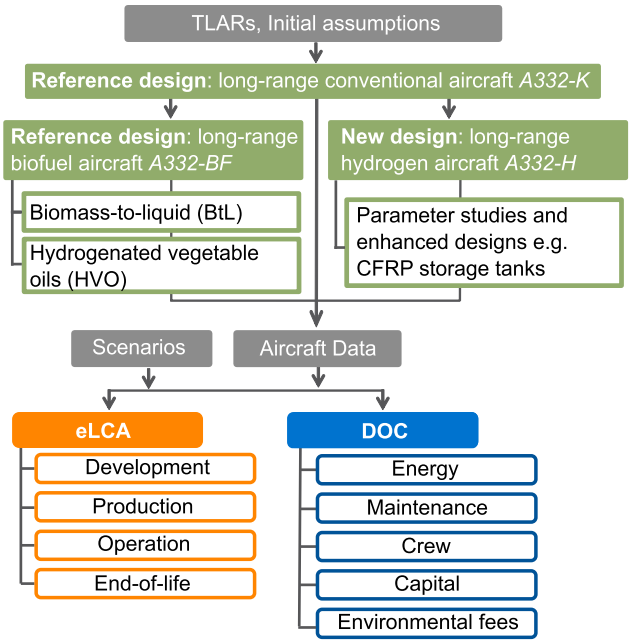

Fig. 1 Established methodology (green represents the aircraft design part, orange the life cycle assessment, and blue the direct operating cost part)

aim of the study is to determine whether, and under what circumstances, hydrogen and biofuel aircraft represent viable solutions for reducing the aviation industry's climate impact from both an environmental and economic perspective.

2 Methodology

The proposed methodology is outlined in Fig. 1 and the general structure of this chapter described in the following.

At first, as shown in Fig. 1, top-level requirements (TLARs) and initial assumptions have to be set. Based on that, the aircraft can be designed, which is explained in Sect. 2.1. A representative long design range is chosen as a TLAR, since the voluminous fuel loads represent a limit to performance improvements for hydrogen aircraft. Therefore, using the in-house aircraft design environment Aircraft Design Box (ADEBO) [8], a long-range conventional transport aircraft powered by kerosene was designed as a reference based on the Airbus A330-200 and abbreviated as *A332-K*. For the drop-in biofuel, the aircraft design remains unchanged and within this study, the aircraft is abbreviated as *A332-BF*. To introduce hydrogen as a propellant, the aircraft requires a new design due to reinforced existing components and additional new components e.g. hydrogen storage tanks. The long-range hydrogen aircraft is abbreviated *A332-H*.

Based on the aircraft data and different scenarios (e.g. electricity mix and fuel costs), in Sect. 2.2 the eLCA methodology is described for all three configurations. First, the general setup of eLCA is explained. Then, the adaptions for the two biofuels, which base on algae and are produced with the biomass-to-liquid (BtL) or the hydrogenated vegetable oils (HVO) processes, are examined. The eLCA adjustments for hydrogen including its production and combustion are also explained. In parallel, a DOC model is applied, which is explained in Sect. 2.3.

For each section, a summary is added at the end to outline the assumptions. Additionally, due to the high demand for assumptions, sensitivity analyses are essential. Parameters are highlighted though out the following sections and examined in Sect. 3.

2.1 Aircraft design with ADEBO

To ensure an efficient and consistent aircraft design process, computer-based programs are established. An example of an aircraft design environment is ADEBO by the Chair of Aircraft Design at the Technical University of Munich. It has been developed for the conceptual design and the early-stage preliminary design of transport aircraft, unmanned aerial vehicles, and fighter aircraft for application in research and teaching. ADEBO is based on an object-oriented data model written in MATLAB and offers high flexibility and extensibility due to its modular structure. Based on an iterative design process, the aircraft is designed with a set of initial assumptions such as, e.g., the geometry, propulsion, aerodynamic settings, and TLARs such as, e.g., the design range or payload mass. The aircraft is initially sized with the design chart to determine the important performance parameter thrust-to-weight ratio and wing loading. Also, a mission analysis tool based on [9] is executed calculating the required fuel mass and the operating empty mass. Subsequently, the aerodynamic calculation is refined and the main aircraft components (wing, fuselage, tail, engines) are sized. Then, they are arranged to ensure stability and their masses determined. When the design reaches the convergence criterion (here maximum take-off weight), the process is terminated. Detailed information about ADEBO is given in [8].

All designs are undertaken using ADEBO and are described in the following. In Sect. 2.1.1, the design process of the A332-K and its initial assumptions are described. Sect. 2.1.2 explains in detail why the aircraft

Table 1 Top-level aircraft requirements and initial assumptions for the A332-K

	Description	Assumption	Refs.
TLARs	Number of passengers	293	[10]
	Payload mass	37923 kg	[11]
	Design range	5500 NM	[12]
	Cruise Mach number	0.82	[13]
Initial assumptions	Entry into service (EIS)	2040	[1]
	Cabin layout	Single deck, double aisle	[11]
	Cruise altitude	11887.2 m	[10]
	Thrust specific fuel consumption	1.6 10^{-5} kg/s N	[14]
	Wing aspect ratio	10.06	[11]
	Wing taper ratio	0.23	[11]
	Aircraft certified noise levels:		
	Sideline	97.36 EPNdB	[15]
	Flyover	90.33 EPNdB	[15]
	Approach	96.74 EPNdB	[15]

design for the A332-BF and A332-K is the same. In Sect. 2.1.3, the A332-H design methodology is given including the general information on hydrogen as an energy carrier, the selection of the storage tank, its design, and the required design adaptions. In Sect. 2.1.4, a summary is added to outline the assumptions of the designs.

2.1.1 Kerosene aircraft design

The design process of the A332-K follows a methodology similar to the one explained in [8]. TLARs and initial assumptions for the aircraft design are listed in Table 1.

First, the TLARs are shown: The payload mass was selected according to the actual payload-range diagram of the A330-200 [11] and a selected design range of 5500 NM. It comprises the capacity of 293 passengers in a two-class layout, a mass of 111 kg per person (including baggage) [16] and an additional freight mass of 5400 kg (excluding the nine crew members [17]). The cruise Mach number was also set based on current data [13].

Additionally, the initial assumptions are listed: As the earliest hydrogen-fueled aircraft can be expected to commence routine operations around 2040 [1], the technology level for all aircraft designs was adapted accordingly and implemented as weight reductions. A technology improvement of 16% compared to the A330-200 from 1998 (initial service date [10]) has been applied to individual component weights based on [18] in addition to a 10% future weight reduction on the furnishing. Parameters, such as the cruise altitude or the aspect ratio, were inherited from the A330-200 to avoid drastic geometrical or operational changes compared to the reference aircraft. The initial long-range cruise altitude is set to 39000 ft or 11887.2 m and is required for, e.g., the fuel mass calculation or the environmental impact assessment. Furthermore, the thrust-specific fuel consumption (TSFC) for the kerosene-powered aircraft is assumed based on the engine Trent 772B [14]. The geometrical properties wing aspect ratio and taper ratio are taken from the aircraft characteristics manual of the A330 and are set constant within the design loop. Lastly, the noise properties come from the Noise Rating Index of the Airports Council International [15], which are needed for the economical assessment.

2.1.2 Aircraft design utilizing biofuels

The development of SAFs is currently receiving increased attention. Possible fuels include biofuels based on vegetable oils, and advanced biofuels made from, e.g., algae or synfuels synthesized from H_2 and CO_2, which require different production processes [6]. The advantage is that they entail few or no changes in the aircraft design and fuel infrastructure. Minor changes are expected in payload and range because SAFs have a different chemical composition (e.g. lower aromatics). As shown in Fig. 2, they tend to have a higher lower heating value (LHV) and lower density compared to Jet A. The data shown are for different SAFs from [19, Fig. 4] (referred as *synthetic paraffinic kerosene* in [19] which can be produced by hydrotreating like HVO and FT pathways like BtL) and for the nominal Jet A from [20].

In this study, the fuel is an advanced algae biofuel as considered in the eLCA of Johanning [22]. It is assumed that the biofuel's gravimetric and volumetric energy density is comparable to the kerosene's density and that the changes in the payload-range diagram are negligible. Therefore, the A332-BF design process follows the A332-K methodology. As the production pathway, the emissions, and the costs of biofuel are not relevant for

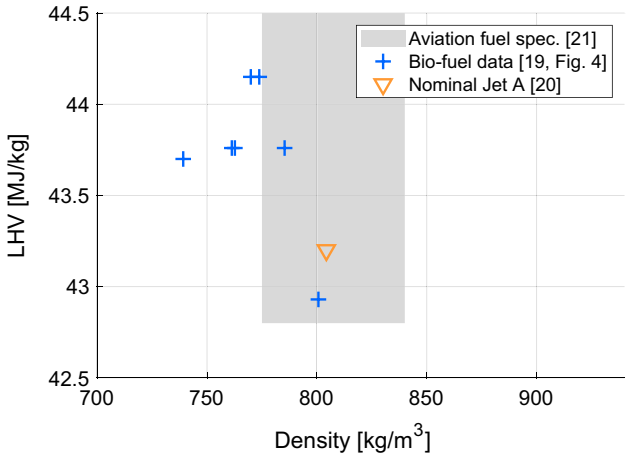

Fig. 2 Relationship between LHV and density for various synthetic paraffinic kerosene relative to aviation fuel specification ASTM D-1655 [21] (densities at 15 °C), adopted from [19, Fig. 4]

the design, it is referred to Sects. 2.2.1 and 2.3.1 for more information.

2.1.3 LH_2 aircraft design

In addition to the development of new propellants, disruptive design concepts offer the opportunity to meet the goal of reducing environmental impact. These concepts include propulsion technologies such as hydrogen for direct combustion in gas turbines or fuel cells that power electric motors. Within this study, the direct combustion of hydrogen is addressed in more detail.

Using hydrogen instead of kerosene has a significant impact on the aircraft's design and performance. To understand these changes, the following is considered:

- Sect. 2.1.3.1: H_2 is considered as an energy carrier with its advantages and disadvantages.
- Sect.2.1.3.2: Since the H_2 tanks are the most challenging new design component, a detailed review of the storage tank options (position, arrangement, geometry, structure, and insulation) are provided.
- Sect. 2.1.3.3: To ensure safe operation, the tank must be thermally and mechanically designed.
- Sect. 2.1.3.4: The effect on the aircraft design process and different components such as on the fuselage, wing, and systems is explained.

2.1.3.1 Hydrogen as fuel Hydrogen is the most abundant element on earth comprising approximately 75% of all matter by weight, whereas it only exists in molecular form and as a compound such as in water [23]. With the extraction of the molecular hydrogen H_2, e.g., by removing the oxygen in the water, it can be used as an aircraft fuel. In the following hydrogen and H_2 will be used synonymously.

Table 2 Properties of liquid hydrogen and kerosene, adapted from [2]

Properties	Hydrogen	Kerosene
Nominal composition	LH_2	$CH_{1.93}$
Liquid density[a] (g/cm^3)	0.071	0.811
Boiling point at 1 atm (K)	20.27	440–539
Specific heat ($J/(g\,K)$)	9.69	1.98
Specific energy (kJ/g)	120	42.8

[a]For hydrogen at boiling point, for kerosene at 283 K

To illustrate the potential of H_2, Table 2 compares some physical properties of liquid hydrogen and kerosene.

The first two listed properties show disadvantages of LH_2. It is 11.4 times less dense than kerosene, resulting in 4.1 times more volume required based on the specific energy. The designer has the difficult task of integrating this fuel volume in- or onto the aircraft. A comparison is only made for the liquid phase because the gaseous storage option is impractical due to its four times lower volumetric energy density [24]. Other storage forms such as supercritical LH_2, carbon nanotubes, or metal-organic frameworks are either heavy or have not yet been sufficiently researched [1, 25, 26]. Moreover, LH_2 must be stored cryogenically because of its boiling point. This leads to the requirement of a tank structure with a minimum surface-to-volume ratio to minimize heat leak and structural weight. The cryogenic property is accompanied by a tank system that must provide pressurization, venting, and insulation. Also, a slight overpressure, e.g. 1.45 bar, is required to prevent the ingress of ambient gases while increasing the structural stability of the tank [27, p.11] [2].

The last two properties are advantages. The greater specific heat of H_2 in comparison with kerosene provides significant cooling capacity. For example, the fuel can be used as a heat sink to cool the engine and other systems. Promising technologies to improve the overall engine cycle efficiency are compressor pre- and intercooling or turbine cooling. With LH_2 and a heat exchanger, the bleed air required for the turbine taken from the compressor could be reduced or eliminated and additionally increase the turbine entry temperature. In addition, hydrogen is more energetic than kerosene. Overall, it has 2.8 times more energy per kg, resulting in a reduced TSFC [2].

Besides the positive and negative effects due to its physical properties, LH_2 has drawbacks for off-design missions. If a shorter distance than the design range is flown, the tank volume will not be fully utilized and thus unnecessary tank weight carried. If the design range is exceeded, the payload must be greatly reduced due to the limited tank capacity [27,

p.7]. Within this conceptual aircraft design study, off-design missions are not considered.

Another aspect that often arises in relation to hydrogen is the importance of safety. It is generally believed that hydrogen is a very hazardous fuel since the accident of the airship Hindenburg. However, there are several studies proving that it can be operated safely. For more information, it is referred to [2, 3, 28].

2.1.3.2 Selection of the hydrogen tank configuration and materials The LH_2 storage tanks are the most challenging new components in the design of hydrogen aircraft. Several assumptions are necessary before starting the actual structural and thermal tank design, such as the tank position, arrangement, geometry, structure, and insulation type.

Tank position Within this study, the tanks are integrated into the aircraft. The physical properties (low volumetric density and minimum surface-to-volume ratio) are one reason. The other reason is safety: In [2, Chapter 8], preliminary investigations of the crash hazard and tank vulnerability were conducted. They found out that LH_2 tanks are less susceptible to damage located in the fuselage than in the wing (such as for the current Jet A tanks). A reason for that is the significant amount of structure around the tank can absorb the impact loads. Additionally, LH_2 is found to be a safe fuel as in case of a tank rupture, hydrogen evaporates and dissipates rapidly, posing little risk to the surrounding environment.

Therefore, there are two general tank position arrangements for long-range hydrogen aircraft: top tanks and front-and-aft tanks [29]. Top tanks cover the entire cabin length and have a diameter equal to 50% of the fuselage. A tail tank is added when the mission requires more tank capacity. For the front-and-aft tanks, one tank is located behind the cockpit and one behind the classical cabin section. A tank cutout is discussed to include a cockpit-cabin interconnection, which would eliminate the need for a separate cockpit door and give the captains the possibility to inspect the cabin. However, there is currently no regulation that imposes such an interconnection. Additionally, the separation will lead to different door, toilet, galley, and crew rest compartment positions, but it is believed that both options would have similar weights [1, 4].

In an analysis, Verstraete explored the impact of the configuration choice for short- and medium-range aircraft. He identified a considerable increase in tank weight for top tanks [29]. Another investigation was presented by Troeltsch et al. for a long-range aircraft [5]. The results showed that the lowest relative fuel consumption is for the front-and-aft tank configuration (see also [2, 30]).

Therefore, the front-and-aft tank configuration is considered in this study. To position the center of gravity appropriately, it is assumed that the front tank contains 40% of the total fuel [4].

Tank arrangement Additionally, a basic distinction is made between non-integral and integral tank arrangements. Non-integral tanks are supported within the conventional fuselage structure. They are designed to take only loads associated with containment of the fuel, e.g. pressure loads, fuel dynamic loads, and thermal stresses. In contrast, integral tanks are integrated into the aircraft structure and include the fuselage frame inside the tank. In addition to the mentioned loads, they must be capable of withstanding all the axial, bending, and shear stresses of the fuselage [2, 27, 31]. Considering the conceptual design of the LH_2 aircraft, the non-integral tank concept is selected as it does not require detailed information about the fuselage geometry or loads, and no structural changes to the fuselage frame are needed.

Tank geometry Another aspect to be considered is the tank's shape. Theoretically, the optimum tank shape is a sphere, because the stress and strain are uniformly distributed and the surface-to-volume ratio is the lowest. Due to the difficulty in manufacturing, large-sized spherical containers are expensive [32]. Considering tanks located inside the fuselage, using one spherical tank would lead to a high fuselage diameter while using multiple small tanks would increase their total mass. Therefore, a cylindrical tank shape for the front tank and a conical shape for the aft tank are preferred. Here, it is also important to investigate the shape of the end closure of the tanks. Brewer [2] studied three possible dome-shape configurations depicted in Fig. 3. The result was that hemispherical domes were the least efficient in terms of cost and the elliptical and the torispherical domes offered approximately equal DOC. The torispherical tank end configuration was chosen for this study.

Tank structure The choice of structure is the next feature to be considered. As a FAR requirement demands that each engine must be supplied with fuel from a separate tank during take-off, a bulkhead is provided in each tank to split it physically in two. The bulkhead material is chosen to be the same as for the tank's pressure vessel [2]. The pressure vessel is directly exposed to the fuel and hence the material choice plays a major role in providing a safe and reliable

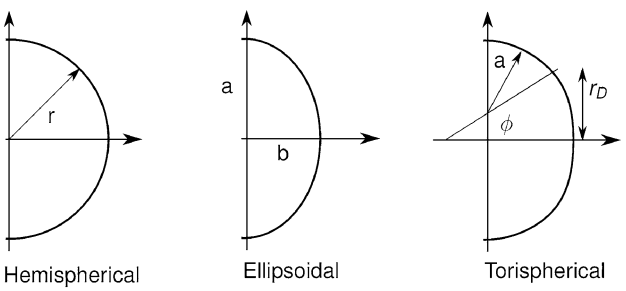

Fig. 3 End closure configurations, [33] adapted from [2, Figure 4-72]

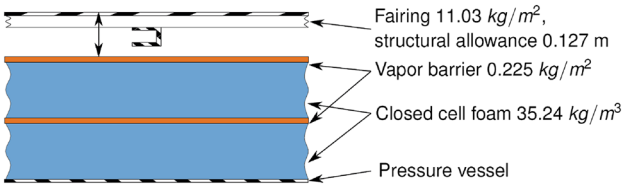

Fig. 4 Non-integral tank design with a rigid, closed-cell polyurethane foam insulation applied to the exterior of the tank wall and two vapor barriers, [33] adapted from [2, Figure 4-79]

structure. The key characteristics of the material include the cryogenic temperature, H_2 permeation, and material embrittlement. Mital et al. report that potential wall material candidates are monolithic metals as well as composites and hybrid constructions such as metal matrix composites [34]. Since hybrids are not widely used in cryogenic tanks, they are neglected here. As the use of composite materials offers a weight advantage over conventional metallic designs ([35], 30% weight saving), they are considered as the reference tank material within this study. The selected baseline material is IM7/977-2, which is already used in space applications for cryogenic tanks. The major disadvantage of composites is their high H_2 permeation. Therefore, Schultheiß recommends a 1 mm aluminum liner, which reduces H_2 permeation to an acceptable level [36]. Possible metals that show acceptable properties under cryogenic conditions are austenitic stainless steels, titanium, and aluminum alloys. Aluminum alloys show only minimal susceptibility to hydrogen embrittlement, and have a lower density than steel or titanium. Brewer performed an extensive study of the mechanical design of the tank wall and recommended aluminum Al 2219 T851 [2] (see also [4, 27]). This material is considered in a parameter study in Sect. 3.4.

Tank insulation The last important point in tank design is the insulation[1]. Here, the main objective is to maintain the cryogenic temperature and minimize boil-off for a minimum increase in weight. By keeping the tank in a 'cold condition', the extreme thermal cycling of the tank structure is limited. The broad classes of possible aerospace cryogenic insulation systems include vacuum jackets, foams, perlites, aerogels, and multilayer insulation (MLI) systems. In this study, the foam-based insulation shown in Fig. 4 forms the basis for the LH_2 tank design. A detailed discussion is outside the scope of this study but is covered in [2, 4, 34].

2.1.3.3 Hydrogen tank design The overall objective is to ascertain the dimensions and the total mass of the tank based on the fuel weight and the necessary tank volume. The driving tank properties are the tank wall thickness ensuring that the tank withstands the applied loads and the insulation thickness regulating the heat flux which can be determined with mechanical and thermal design models. In the next sections, a general introduction to the compromise of these models is given followed by details about the mechanical, thermal design, and sizing methods.

General setup The influence of the loads and the effectiveness of the insulation must be considered in several operating cases: the first case is the in-flight operation. During the flight, the pressure will rise in the tank due to the heat entering through the insulation, resulting in the conversion of LH_2 in GH_2. However, the pressure will fall due to fuel consumption in flight. If the system were optimally designed, i.e. with optimum insulation and corresponding fuel consumption, evaporation losses would be avoided. However, operating on ground will lead to a large increase in pressure due to the heat input without a counteracting effect, as the aircraft is fully fueled without consuming fuel. Therefore, the tank design must ensure that the tank operates safely despite the varying pressure in-flight and increasing pressure on the ground. According to Brewer, H_2 vented on ground can be recovered very economically, however, the quantity vented during flight is of major concern because it is simply lost [2, p.164-165]. In this study, a similar approach to that outlined in [2] and [27] is adapted: the absolute pressure in the tank is kept constant, thus ensuring that there is no risk of collapse or overpressurization. When the pressure decreases, LH_2 is converted into GH_2 with the proposed tank pressure generation system [2, Ch. 4.3.2]. When the pressure in the tank exceeds the maximum tank pressure, the excess gaseous hydrogen has to be vented.

Mechanical design With the approach of constant absolute tank pressure, the tank pressure vessel and therefore the tank wall thickness can be calculated. As non-integral tanks have been selected, they only have to sustain the loads associated with fuel containment. In this design phase, insufficient data are available to consider all of these loads and a detailed finite element analysis is not feasible within the scope of this work. The tanks are thus designed based on an analytical approach (ASME Boiler and Pressure vessel code) for the pressurization loads including safety factors to account for the other loads [2, 4, 37]. This approach requires assumptions for the storage pressure and the allowable stress of the tank material.

The recommended storage pressure is at 21 psi or 1.45 bar. The highest differential pressure acting on the tank occurs at the highest cruise altitude. The differential pressure is multiplied by a factor of 1.1 to allow for relief valve tolerance and inertia effects, and a factor of 1.5 to allow for fuel dynamic loads. [2, p.155]

As the design loads are known, the allowable stresses can be determined to calculate the wall thickness. Table 3 summarizes the properties of aluminum Al 2219 T851 and

[1] Insulation also has to be applied to the fuel supply system. The implementation is described in 2.1.3.4.

Table 3 Properties of different tank wall materials [2, Table 4-19], [40, p.4], [41, 42]

	CFRP IM7/977-2	Aluminum 2219 T851
Density (kg/m^3)	1565[a]	2850
Hoop strength (MPa)	375[b]	172
Permeability	High[c]	Low

[a] In literature: 1530–1600kg/m^3.

[b] In literature: 600–2690MPa (high uncertainty). With assumption for −30% weight, strength value was adjusted based on ASME formula.

[c] Can be reduced by using a thin aluminum liner

CFRP IM7/977-2. It shows that the range of CFRP density and strength values found in the literature is very wide. Additionally, it must be taken into account that formulas such as the general calculation of a cylindrical pressure vessel based on ASME have been developed for isotropic materials [38, p.412-3]. The same applies to the dimensions of torispherical heads, which are given in [39]. However, for composite materials, the allowable stresses depend on the particular laminate and would have to be determined by testing or by conservative estimates based on the previous testing of similar laminates. As the maximum circumferential stress data are uncertain, the assumption of a 30% weight reduction compared to the aluminum tank is taken as a basis. Using the general ASME formula from [38, p.412-3], the strength assumption was adjusted to match the weight reduction.

Thermal design To estimate the insulation thickness, a simplified thermodynamic model adapted from [27] was implemented in ADEBO. The chosen use case is a tank filled to 98% capacity (2% ullage filled with GH_2 [2, p.31]) designed under on-the-ground conditions. The mean outer temperature T_o is set to 290K [2, Table 4-30]. The temperature of the liquid T_{LH2} is 20K, equal to the maximum boiling point. The vapor temperature near the liquid T_{GH2} is considered to be 36K [2, Table 4-29].

It is assumed that heat is lost from the tank via the heat loss flow $\dot{Q}$ which is equal to the evaporating mass flow $\dot{m}$ multiplied by the specific enthalpy of vaporization h_v:

$$\dot{Q}[\mathrm{J/s}] = \dot{m}[\mathrm{g/s}] \cdot h_v[\mathrm{J/g}] \tag{1}$$

with $\dot{m}$ set equal to 0.167% by weight per hour of the fuel mass [5]. The specific enthalpy of vaporization is the sum of the specific enthalpy of LH_2 $h_{v,LH2} = 446\mathrm{J/g}$ at the boiling point [4, Table A.1] and the increase in the enthalpy due to the temperature difference relative to GH_2 $\Delta h_{v,GH2}$:

$$\begin{aligned} h_v[\mathrm{J/g}] &= h_{v,LH2}[\mathrm{J/g}] + \Delta h_{v,GH2}[\mathrm{J/g}] \\ &= h_{v,LH2} + c_p''[\mathrm{J/(g\ K)}] \cdot (T_{GH2} - T_{LH2})[\mathrm{K}] \end{aligned} \tag{2}$$

with the specific heat capacity of saturated H_2 steam $c_p'' = 12.5\mathrm{J/(g\ K)}$. The ullage filled with GH_2 is neglected:

$$\dot{Q}[\mathrm{J/s}] = A_m[\mathrm{m^2}] \cdot \frac{\lambda_{\mathrm{Insu}}[\mathrm{W/(mK)}]}{t_{\mathrm{Insu}}[\mathrm{m}]} \cdot (T_o - T_{LH2})[\mathrm{K}] \tag{3}$$

with A_m as the mean lateral surface area of the tank and λ_{Insu} as the thermal conductivity of the selected polyurethane closed cell foam insulation. The thermal conductivity was chosen as $20 \cdot 10^{-3}\mathrm{W/(mK)}$ with a mean wall temperature of 155K ([4, p.52], [2, Figure 4-78]).

It appears straightforward to determine the tank size once the tank layer thicknesses and the fuel volume are known since the tank is constrained in its diameter due to the fuselage. However, the insulation thickness depends on the lateral surface area (see Equation 3) meaning that with increased fuel mass, the insulation thickness changes influencing the inner tank volume, total length, the aircraft's maximum take-off weight, and subsequently the fuel mass again. Therefore, the sizing method is a highly iterative method requiring a convergence loop. Additionally, a factor of 3.8% is applied to the fuel volume to account for net tank contraction or expansion due to cooling and pressurization, internal structure and equipment, trapped and unusable fuel, and ullage[2] [2, Table 3.4].

The total tank mass can be calculated based on the overall dimensions. The tank consists of: the pressure vessel (an aluminum alloy liner of 1 mm is applied for a CFRP pressure vessel), insulation, vapor barrier, bulkhead, and fairing. The masses are determined based on the volume or surface area and the material density (see Fig. 4).

Due to the high amount of uncertainties, the tank mass, respectively gravimetric storage efficiency $\eta_{\mathrm{grav,tank}}$ (ratio of fuel mass to the sum of fuel and tank mass), is varied in a parameter study. The Clean Sky report assumed 0.38 for the tank efficiency specifically for long-range [6]. This is in range with Huete et al. assuming an interval from a pessimistic 0.3 to an optimistic of 0.85 [43]. To understand the sensitivity, this is considered in a parameter study.

2.1.3.4 Aircraft design process adaptions Additional adaptions for the A332-H are required: First, as the fuel tanks are located inside the fuselage, the total length of the LH_2 aircraft could exceed the 80m gatebox constraint or lead to tail scrape problems at take-off. A double deck layout can shorten the fuselage as it reduces the cabin length by placing the passengers on a second deck. Furthermore, this configuration leads to an increased fuselage diameter that is beneficial in terms of shorter hydrogen storage tanks. Thus,

[2] The volumetric allowance for boil-off is not included, as it is already considered in the thermal design [2, Table 3.4].

within this study, a double deck layout is implemented for the A332-H.

One of the most important advantages that LH_2 offers is its high LHV which results in 2.8 times less fuel required. Therefore, the TSFC stated in Table 1 for A332-K is reduced to 0.571 10^{-5}kg/(sN) for A332-H.

For conventional aircraft, the fuel is stored, among others, in the wing. The fuel mass reduces the root bending moment generated by lift. As for H_2 in-fuselage storage is necessary, but the bending moment and flutter effect still occurs, the wing must be reinforced to withstand these effects. Verstraete evaluates the magnitude of weight increase using the inertia relief factor according to [44]. He estimates an overall wing weight increase of 6% [18].

The fuselage of the LH_2 aircraft needs to be reinforced as the two tanks exert additional point loads on the structure. This leads to an estimated 6% increase in fuselage mass [2, p.22, 36-37].

Another change is the more complex fuel supply system. The fuel pipes must be insulated in the same way as the tanks to ensure steady fuel flow. Brewer recommends adding 80% to the Jet A fuel system mass estimation method [2, p.37].

If the pressure in the tank exceeds the nominal pressure, the fuel must be vented. Therefore, a trip fuel loss of 1.375% has been introduced [27, p.160]. The percentage value was estimated based on the fraction of the densities of the vented gaseous phase relative to the stored liquid phase. Due to the uncertainties associated with this estimation, the influence of this value was explored in a parameter study ranging from 0 to 2.75% in Sect. 3.4.

2.1.4 Summary

Following design assumptions are made: A332-K is a long-range conventional powered aircraft with an EIS in 2040. The biofuel (fresh water microalga) is considered a drop-in and consequently, no design changes are required. For the hydrogen-powered aircraft A332-H, significant changes in the design are made including the most challenging hydrogen tank integration. The assumptions are summarized in Table 4.

2.2 Environmental life cycle assessment model

Environmental life cycle analyses are a widely used tool in determining the environmental impact of aircraft. They incorporate not only the operational phase of an aircraft but also, among others the fuel production, providing a complete picture of the environmental impact. Several eLCA's of aircraft have been carried out, e.g., [22, 45–48]. Due to its free availability and its ability to analyze kerosene-, biofuel- and H_2-powered aircraft, the model by Johanning is used in this study [22]. It is a comprehensive eLCA model that integrates easily into the aircraft design process. The following gives an overview of the method with a focus on biofuel and hydrogen aircraft. A detailed description of the complete model can be found in [22].

According to DIN EN ISO 14040, an eLCA consists of four steps: (1) goal and scope definition, (2) inventory analysis, (3) impact assessment, and (4) interpretation of the results. In this study, the goal and scope is the comparative analysis of different civil aircraft concepts in terms of their environmental impact from cradle to grave. The aircraft life cycle is shown in Fig. 5 is split into four main phases: the design and development (includes, e.g., the electricity needed for the computer use), the production (includes, e.g., the resources required and emissions during the material production), the operation (includes, e.g., what is emitted during cruise) and end-of-life (includes, e.g., material of the aircraft that can be reused).

The inventory analysis of Johanning's model is primarily based on the EU's ELCD database. For the impact analysis, the ReCiPe 2008 method[3] is employed. It calculates the environmental impact of the aircraft in terms of a so-called single score (SS) [points/ passenger-kilometer] based on the results of the inventory analysis. The SS is the aggregation of three endpoint categories (damage to human health, ecosystem diversity, and resource availability) or 18 midpoint categories (e.g. climate change, ozone depletion, water consumption, land occupation, particulate matter formation, etc.). The uncertainties increase from the inventory analysis, over midpoint and endpoint categories, to the single score. They are addressed via different weightings, perspectives, and regions that group distinct sources of uncertainty and choices [52]. In this study, the region *world*, the perspective *hierarchist*, and the *average* weighting are chosen for the reasons outlined in [22, p.28].

There are two aspects that need to be considered in the evaluation when switching from short-haul to long-haul. First, the number of aircraft in a family is smaller. Johanning recommends a size of 20000 for short-haul and 2000 for long-haul [22, p.31], which is consistent with Airbus' data (currently 2087 aircraft of types A330/A340/350, [53]). Secondly, the total duration required for the ground handling of an aircraft differs for the aircraft categories light, medium and heavy [54, p.22]. For the A330-200, and respectively the A332-K, a ground handling time of 75min is selected.

In the following, the adjustments of the eLCA method by Johanning to account for biofuel and LH_2 are outlined in

[3] The ReCiPe 2008 method was enhanced by Johanning in the midpoint category *climate change* takes into consideration persistent contrails, contrail cirrus, and NO_x effects of aircraft on climate. The altitude-dependence of these effects is based on 1D climate functions from the LEEA project [50, 51].

Table 4 Summary of A332-H design assumptions

		Assumption/value	Refs.
Tank configuration	Position	Front-and-aft tanks (40–60%)	[1, 2, 4, 5, 29]
	Arrangement	Non-integral	[2, 31]
	Geometry	Cylindrical & conical shape with torispherical heads	[2]
	Structure	CFRP (IM7/977-2) pressure vessel with aluminum liner (Al 2219 T851) & integrated bulkhead	[2, 4, 27, 34–36]
	Insulation	Polyurethane closed cell foam and vapor barriers	[2, 4, 34]
Tank design	Mechanical	Storage pressure at 1.45bar (multiplied by 1.1 and 1.5 as safety factors)	[2]
	Thermal	$20 \cdot 10^{-3}$W/(mK), 2% ullage, 3.8% safety margin	[2, 4, 27]
Others	Fuselage	Double-deck	
	TSFC	0.571 10^{-5}kg/(sN)	
	Wing mass	+6%	[18]
	Fuselage mass	+6%	[2]
	Systems mass	+80%	[2]
	Trip fuel loss	Additional 1.375%	[27]

Sect. 2.2.1 and Sect. 2.2.2, respectively. At the end of this section, a summary is added in Sect. 2.2.3 to outline the assumptions of the eLCA.

2.2.1 Adjustments for Aircraft utilizing Biofuels

As described in Sect. 2.1.2, the biofuels considered within this study are assumed to be drop-in (therefore no changes to the aircraft itself) and they are expected to have lower aromatics (meaning different combustion emissions). This means that only the eLCA processes for fuel production and fuel combustion during operation have to be adopted.

Johanning considers two different biofuels in his work [22, 55]: one produced via the BtL process using FT synthesis, and the other by HVO via the process of the Universal Oil Products Limited Liability Company. Both processes are based on the use of fresh water microalga *Auxenochlorella protothecoides* as biomass. The processes are shown schematically in Fig. 6. Both biofuel production processes consist of the cultivation of the microalgae, harvesting, raw material extraction and refinement, and the fuel production itself. While the cultivation is the same for both processes, the algae harvesting used in the HVO process consists solely of preconcentration, but not of cell disruption and dewatering as in the BtL process. As the BtL process requires dry biomass and the HVO oil for the fuel production step, the raw material extraction and refinement are also different. Gehrer provides input data on both processes in her work [56], which Johanning used in his eLCA to produce the input and output values for the production of 1 kg biofuel. Including two electricity mix options (current EU mix and renewable electricity production), four different biofuel options exist in the eLCA (see Table 5). Note here, that the HVO (renewable) production process only requires CO_2 input. This is due to the fact that Johanning uses a cut-off criterion of 2.5% (meaning that only substances with a high impact are considered) to reduce the number of in- and outputs.

Different results have been reported in the literature regarding the combustion emissions of biofuels. However, most studies agree that soot emissions are reduced, which is attributed to the lower aromatics content (and therefore higher hydrogen-to-carbon ratio) of biofuels. In turn, the higher hydrogen-to-carbon ratio leads to an increase in H_2O emissions, but also to a reduction in combustion temperature, which is favorable for lower NO_x emissions. While reported results of CO and HC emissions of biofuels are conflicting, Blakey et al. state that it is likely to be linked to the content of aromatics of the fuel. Due to the larger LHV of biofuels (see Fig. 2), less fuel is required for the same mission, and, since CO_2 emissions are directly proportional to the fuel flow rate, they are reduced. [19, 20, 58–60]

Recently, Voigt et al. reported on their experiments with a biofuel-powered A320 in respect of concerning contrail

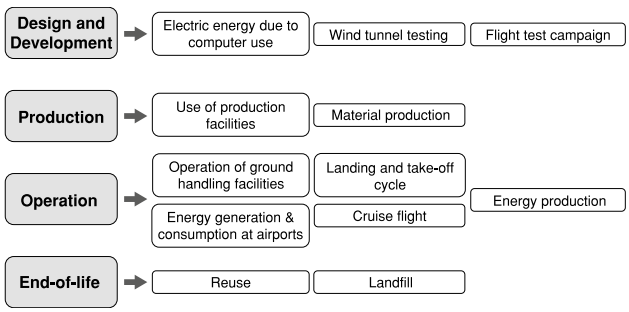

Fig. 5 Aircraft life cycle processes incorporated in the model [22, Fig. 3.3], taken from [49]

Table 5 In- and outputs in g for the production of 1 kg biofuel [22, 55]

	Hard coal	CO_2	Natural gas	Crude oil	CH_4	Brown coal	SO_2
BtL (EU mix)	9780.0	44400.0	3530.0	1680.0	0.0	0.0	0.0
BtL (renewable)	36.2	− 698.0	120.0	161.0	3.1	29.5	0.0
HVO (EU mix)	3543.0	13475.0	1800.0	741.0	0.0	5097.0	143.0
HVO (renewable)	0.0	− 9743.0	0.0	0.0	0.0	0.0	0.0

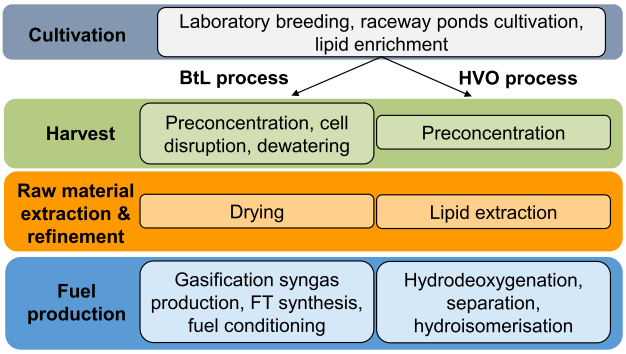

Fig. 6 BtL and HVO process based on [56, Fig. 2], [57, Fig. 1]

cloudiness. They found that the use of biofuels with a low aromatics content reduced soot and ice crystal numbers by 50–70% and increased ice crystal size [60]. This decreased contrail optical depth and lifetime, and thus reducing its radiative forcing [61, 62]. As contrail cirrus is the largest contributor to aviation climate impact [63], this is an important finding. Bock simulated contrail radiative forcing assuming a reduction of 80% in ice crystal number concentration, and found that the radiative forcing would be reduced by 58% [62, Ch. 6].

Nevertheless, it should be considered that (1) the emissions depend on the exact composition of the biofuel, and (2) the experimental studies on biofuel emissions are reporting different reduction/increase potentials. Additionally, it is to be noted that the eLCA methodology does not consider the direct radiative forcing due to soot emissions, however, intrinsically includes them in the persistent contrail and contrail cirrus 1D climate functions derived for kerosene-burning aircraft by [50, 51]. A reduction in soot emissions is coupled with a decrease in radiative forcing of persistent contrails and contrail cirrus, as they act as condensation nuclei in their formation.

In conclusion, and especially based on [61] and the latest personal communication with the authors, a baseline of 40% reduced contrails and contrail cirrus radiative forcing was chosen. The uncertainty is considered in a parameter study between 0 and 60% reduction in Sect. 3.4.

2.2.2 Adjustments for LH_2 Aircraft

The adaptions for A332-H involve the LH_2 production and combustion which replace the respective processes in the A332-K assessment. Furthermore, the aircraft material distribution is updated as shown in Table 6. Using the information on the A330-200 provided in [46, Tab. 4.6], the material distribution of the A332-K and A332-H were recalculated. The recalculation was also required for the A332-K because the values given in [22, Table 3.8] do not include the landing gear and engines.

Moreover, a factor of 1.3 was applied to the development costs, which affect the energy consumption due to computer use and therefore the aircraft life cycle process of design and development (see Fig. 5). The research leading to this factor is described in detail in Sect. 2.3.2.

For LH_2 production, Johanning considers two production pathways: steam reforming and electrolysis using renewable electricity. For completeness, the inputs and outputs for these two pathways are reproduced in Table 7.

In contrast to kerosene, the combustion of hydrogen and air produces only H_2O, O_2, and NO_x emissions (see Fig. 7).

While H_2O and O_2 emissions are directly proportional to the amount of fuel ($8.94 g_{H_2O}/kg_{H_2}$ and $7.94 g_{O_2}/kg_{H_2}$), estimating the NO_x emissions of hydrogen turbofans is still a subject of ongoing research. However, Marek et al. from NASA Glenn provide a P3T3-correlation function which was derived based on their experimental data of hydrogen-burning turbofans using lean direct injection. For their injector configuration C4[4] (which performed best of all the tested configurations), the correlation function is as follows [64, Eq. 12]:

$$\begin{aligned} \mathrm{ppmNO}_x[-] &= 9.355 \cdot (143 \cdot P_3[\mathrm{MPa}])^{0.275} \\ &\cdot \phi_{H_2}^{4.12}[-] \cdot \tau^{0.455}[\mathrm{ms}] \cdot e^{\frac{1.8\ T_3[\mathrm{K}]-460}{211}} \cdot 25^{-0.288} \end{aligned} \tag{4}$$

and for their configuration C3:

[4] C4 is based on C3. C3 is a conservative design based on 2005 gas turbine technology (center nozzle and six evenly distributed nozzles around it), whereas C4 replaces the center hole with four small radial jets per injection point.

Table 6 Material distribution of the long-range aircraft in (%)

	Aluminum	Steel	Composites	Titanium	Miscellaneous
A332-K and A332-BF	53.5	19.6	11.6	8.9	6.4
A332-H (Alu tanks)	58.4	15.7	10.0	7.4	8.5
A332-H (CFRP tanks)	55.7	16.2	12.0	7.7	8.4

Table 7 In- and outputs in g for the production of 1 kg LH_2 [22]

	Hard coal	CO_2	Natural gas	Crude oil	CH_4	Brown coal	SO_2
Steam reforming (EU mix)	1003.0	17534.0	510.0	210.0	160.0	1443.0	50.0
Electrolysis (renewable)	11.3	1524.0	0.0	10.4	0.0	28.1	0.0

$$\begin{aligned} \text{ppmNO}_x[-] = 101 \cdot (143 \cdot P_3[\text{MPa}])^0 \\ \cdot \phi_{H_2}^{2.99}[-] \cdot \tau^{0.439}[\text{ms}] \cdot e^{\frac{1.8\ T_3[\text{K}]-460}{547}} \cdot 20^{0.165} \end{aligned} \tag{5}$$

with P_3 and T_3 being the pressure and temperature at engine station three (last compressor exit face), ϕ_{H_2} the equivalence ratio, and τ the combustor residence time.

However, in this work, the NO_x emissions are required to be in g_{NO_x} per kg_{H_2} (emission index). The following equation is used to convert from ppmNO_x to EINO_x (see derivation in Appendix 1):

$$EI_{NO_x}\left[\frac{g_{NO_x}}{kg_{H_2}}\right] = \frac{1 + FA_{H_2}[-]}{FA_{H_2}[-] \cdot 533} \cdot ppmNO_x[-] \tag{6}$$

with FA_{H_2} being the fuel-to-air ratio. From stoichiometric combustion of hydrogen and air follows that $FA_{H_2,\text{stochio}} = 0.0292$ and with $\phi_{H_2} = \frac{FA_{H_2}}{FA_{H_2,\text{stochio}}}$ and it is defined as:

$$FA_{H_2}[-] = 0.0292 \cdot \phi_{H_2}[-], \tag{7}$$

The input data is summarized in the Appendix in Table 15. For C4 this leads to 0.63 g_{NO_x}/kg_{H_2}, and for C3 to 3.14 g_{NO_x}/kg_{H_2} during cruise. While for C3 this value aligns well with the stated 3 g_{NO_x}/kg_{H_2} from in the AHEAD project [65], the EINO_x of configuration C4 is a further 80% lower. Since the EINO_x estimation of hydrogen-burning turbofans is a matter of current research, the baseline EINO_x is chosen to be 3.14 g_{NO_x}/kg_{H_2} during cruise. However, changes in this value and their impact on the final results of the eLCA and the DOC are evaluated in a parameter study in Sect. 3.4.

Contrary to Johanning, who assumed a constant EINO_x of the hydrogen engine for all mission segments, in this study the EINO_x values for the individual mission segments are approximated from the cruise EINO_x. For this purpose, the ICAO landing and take-off emission data and the cruise EINO_x calculated as stated in [22] of the kerosene-burning Trent 772 engine of the A330-200 are used: by assuming the percentage split across the mission segments is similar for the hydrogen-burning counterpart, the individual EINO_x values are calculated from the cruise value. This leads to the results provided in Table 8.

Similarly to the aircraft utilizing biofuels, it is expected that the contrails of H_2 aircraft have a lower optical depth and shorter lifetime [65, 66], however experimental flight test data have yet to be gathered. In the AHEAD project in 2016, a conservative 40% reduction in radiative forcing due to the reduced soot emissions was assumed by Grewe et al. [65]. Due to the uncertainties, the influence of this value was explored in a parameter study ranging from 0 to 60% reduction [65]. In a 2006 study, Ponater et al. found a reduction in contrail radiative forcing of about 11.5% for a pure LH_2 aircraft fleet in 1992 [66, Tab. 6], while in 2005, Marquardt et al. estimated a 18% radiative forcing reduction for a 2015 inventory [67, Tab. 2]. Due to the increase in knowledge about contrail radiative forcing over the past years, the estimate of the 2016 study by Grewe et al. is considered in this work, but also a 0 to 60% reduction potential is investigated in Sect. 3.4.

2.2.3 Summary

To environmentally assess the different aircraft concepts in their life cycles, the eLCA model of [22] is considered in this study. As baseline settings, the EU's ELCD database, the impact assessment method ReCiPe 2008, the region *world*, the perspective *hierarchist*, and the *average* weighting are chosen.

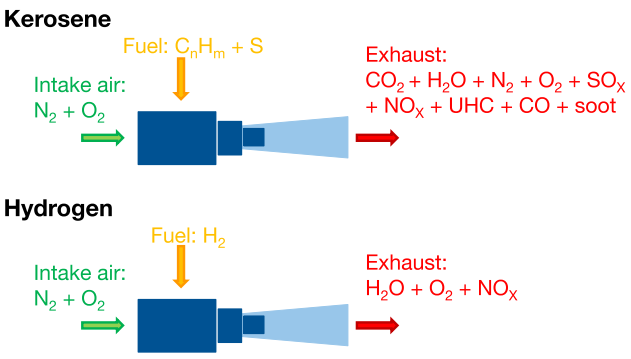

Fig. 7 Combustion of kerosene and hydrogen with air in a gas turbine

The indicator *single score* is used for the relative comparison between the designs.

Minor adaptions for considering the long-range aircraft A332-K are included and different production and combustion paths for the new propellants biofuel and hydrogen are introduced. New material distribution and a factor of 1.3 on development costs for the A332-H are considered.

For the biofuel (fresh water microalga), the BtL and HVO production paths are used. The required electricity can either be based on the current EU electricity mix or renewable energies. The in- and outputs are summarized in Table 6. The combustion of biofuel is similar to kerosene but is assumed to be 40% lower in soot emissions.

LH_2 can either be produced based on methane steam reforming or electrolysis. The in- and outputs are summarized in Table 7. The hydrogen combustion results in only H_2O ($8.94 g_{H_2O}/kg_{H_2}$), O_2 ($7.94 g_{O_2}/kg_{H_2}$), and NO_X (see Table 8) emissions. Additionally, the radiative forcing is assumed to be reduced by 40%.

2.3 Direct operating cost model

A large number of direct operating cost models exist. Among the well-known methods for jet aircraft are the method of the Air Transport Association of America (ATA) from 1967 [68], of Liebeck (1995) which is based on the ATA method [69], of the Association of European Airlines (AEA) from 1989 [70, 71], and the method of the Technical University of Berlin (TUB) from 2013 [72]. Pohya et al. recently compared these methods in terms of the number of required input parameters, covered DOC elements, and results [73]. They conducted that the models differ mainly in (1) the amount of input parameters (e.g., AEA requires 17, whereas TUB model needs 11 inputs) and (2) in the considered cost elements (e.g., ATA does not include airport fees). DOC elements are generally divided into capical (depreciation, interest, insurance), energy, crew, environmental and airport fees, and maintenance costs [74]. These costs are dependent on the airline and its business model or region, which results in high uncertainties of the absolute values available by the empirical functions of the models. However, the DOC models are designed for relative comparison and can provide a general indication of different aircraft types and technologies [68, 73].

The TUB model requires a low number of input parameters, is the only method covering all DOC elements, and has shown good agreement of the absolute DOC value and the DOC element shares [73] with the other methods. For these reasons, the TUB model is chosen as a basis for this study. Several enhancements of the TUB model have been undertaken as summarized in Table 9 and outlined in more detail in [49].

Table 8 NO_x emissions index ($g_{NO_x}kg/_{H_2}$) of the LH_2 long-range aircraft for the different mission segments

Segment	Idle	Take-off	Climb	Cruise	Approach
$EINO_x$	1.10	8.02	6.17	3.14	2.40

- The kerosene price has been updated to the average price in 2019.
- A future kerosene price escalation is included (2.0% p.a. see [75] including, e.g. carbon tax; included in a parameter study).
- An inflation correction is added, permitting the calculation of the DOC for a user-specified year.
- For a complete and meaningful comparison of the concepts, noise, NO_x, and CO_2 charges, levied around the world, are included.

Since the TUB model is only applicable to conventional aircraft, additional modifications accounting for biofuel and LH_2 aircraft have to be undertaken. These are described in the following two subsections and summarized in the last subsection.

2.3.1 Adjustments for Aircraft utilizing Biofuels

Since the biofuel is assumed to be a drop-in fuel, the only necessary change in the DOC model for the biofuel is the price of the fuel. Although lower aromatic and sulfur content of biofuels (and thus lower sulfur compound and particulate matter emissions) could lead to engine maintenance cost reductions [76], in this study a conservative approach is taken and this possible beneficial effect is neglected. Noise and NO_x emissions of the aircraft utilizing biofuels are assumed to be the same as for kerosene-powered aircraft (see Sect. 2.1).

Biofuel price estimations vary widely in the literature and depend, among others, on the production pathway (e.g. FT, hydrodeoxygenation, HVO) and the type of bio-mass (e.g. algae, crop waste, forest product residues). Gehrer or Johanning do not provide data on the BtL or HVO biofuel based on algae and therefore a literature research was conducted. Data on biofuels from different production methods were determined. Fig. 8 summarizes the estimated biofuel cost for hydrotreated (which includes HVO) and FT pathway (which includes BtL) biofuels.

The figure shows that producing biofuels by hydrotreating biomass is cheaper than the gasification-FT pathway. This can be attributed to the fact that gasification-FT is highly capital intensive [81]. Detailed information is listed in the following:

- De Jong concludes that the price for the n[th] production plant is 29.3 €/GJ (ca. 1€/l) for the HEFA pathway (used cooking oil) and 38€/GJ (ca. 1.3€/l) for the FT pathway (forest residues) [77, Fig. 7-1].
- Bann et al. estimated 0.91–1.06$/l (0.80–0.94€/l) for HEFA produced biofuels (biomass: yellow grease and tallow, respectively), and 1.15$/l (1.02€/l) for FT biofuels [78].
- Ram et al. determined the variation of FT biofuel costs around the world in 2050 and concluded that the cost varies between 0.70–1.45€/kg (0.55–1.10€/l) [79, p.224].
- Graham et al. compared the biofuel costs produced with hydrodeoxygenation (1.03AU$/l or 0.64€/l) and gasification-FT (1.41AU$/l or 0.88€/l) in Australia in 2011 [80, Fig. 11].
- Pavlenko et al. calculated the levelized cost of biofuels for different production pathways. Results vary between 0.88–3.44€/l for all considered production pathways (1.34–1.87€/l for gasification-FT pathway, and 0.88–1.09€/l for HEFA pathway) [81, Fig. 2].
- Diego Rojas et al. conducted a survey in 2019 and found near-term biofuel price estimations varying between 1.10 and 4.06€/l, but did not indicate the underlying assumptions (production pathway, biomass type, ...) [82].

Due to uncertainties (e.g., reference year not stated), a conservative value of 2€/l is chosen for both biofuels for the financial year of 2019.[5] The influence of this choice on the results will be explored in a parameter study in Sect. 3.4.

2.3.2 Adjustments for LH_2 Aircraft

For the development of a LH_2 aircraft DOC model, first, a literature survey of LH_2 subsonic aircraft cost models was undertaken. The results are summarized in Table 10.

All surveyed studies used a basic model for conventional aircraft and adapted it to LH_2 aircraft. In doing so, different basic models and adaptions have been pursued. Although most of the studies use a different basic model, the changes compared to the baseline model are similar. All studies have adjusted the fuel price value to reflect hydrogen cost. Most studies have also modified the aircraft price (capital cost estimation) to factor in the increased development costs. Three out of nine studies also changed the engine maintenance cost and/or the airframe maintenance cost. The respective factors are also shown in the table.

As indicated in Sect. 2.3, the basic model chosen within this study is the TUB model, as was also used by [27]. Based on the conducted literature survey, the following changes have been introduced:

[5] With an assumed density of biofuel of 0.77kg/l this translates to 2.6€/kg.

Table 9 DOC model updated values and enhancements

Variable	Value
Kerosene price	0.517 $€_{2019}$/kg[a]
Kerosene price escalation	2.0% p.a.
Unit cost rate noise	2.82 $€_{2019}$/noise unit
Unit cost rate NO_x	3.70 $€_{2020}$/kg
CO_2 allowance price	15.5 $€_{2019}$/t
Portion of auct. emission cert.	0.15

[a] Is equivalent to 80.13 $\$_{2019}$/bbl

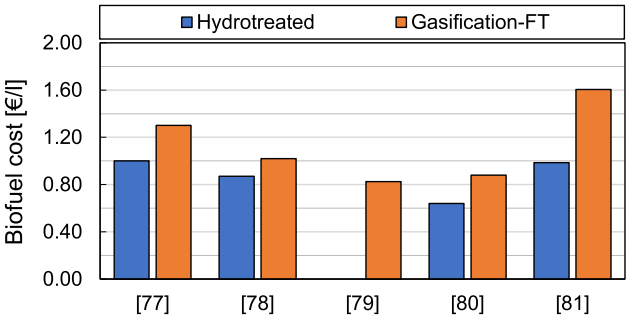

Fig. 8 Biofuel cost estimations in literature for hydrotreated fuels and fuels produced via the gasification-FT pathway (average data from [77–81])

- The fuel price is adopted to a value reflecting the price of LH_2. Fig. 9 shows the results of a hydrogen cost literature survey. The data is quite scattered, but narrows towards 2050. In this study, a LH_2 price of 4.07$/kg is assumed for 2040 (equals 2.66$/kg assumed for 2019). However, due to the uncertainties associated with this value, it is included in a parameter study in Sect. 3.4. Boil-off losses during flight are calculated within the mission performance and taken into account during tank sizing (see Sect. 2.1). They are included in the block fuel mass. In addition, 1.4% refueling losses are taken into account [27, p.160]. Additional electricity and helium costs for pumping the fuel, pressurizing and purging the fueling system are not considered. Mangold calculates the resulting LH_2 price increase to be between 0.45% and 13.62%, depending on the chosen fueling system [87, Tab. 3.4].
- Due to the new technology involved in LH_2 aircraft, allowing for increased development costs and the additional cost of the LH_2 tanks seems reasonable. A factor of 1.3 is chosen based on the literature survey for the aircraft price. However, due to the uncertainty of this factor, it is included in a parameter variation.
- Running gas turbines on hydrogen will eliminate coking and other deposits in the combustion chamber and turbine. Furthermore, more uniform heat distribution in

Table 10 Summary of hydrogen aircraft cost models survey in literature

Refs.	Model used in source	Changes compared to basic model			
		Fuel price	Aircraft price	Engine maint.	Airframe maint.
[1]	No/unknown	Yes, for same DOC	Yes, factor unknown	No/unknown	No/unknown
[2]	ATA	Yes, for same DOC	No/unknown	Factor 0.7	No/unknown
[3]	Burns	Yes, for same energy	Yes, factor unknown	No/unknown	No/unknown
[4]	Liebeck	Yes, for same DOC	Factor 1.1–1.5	No/unknown	Factor $1.1 - 1.5$
[27]	TUB	Yes, incl. losses	Factor ≈ 1.059	Factor 0.7	Factor 1.07 + OEM scaling
[83]	ATA	Yes, incl. boil-off rate	Factor ≈ 1.49	Factor 0.67	No/unknown
[84]	PrADO	Yes	No/unknown	No/unknown	No/unknown
[85]	Unknown	Yes	No/unknown	No/unknown	No/unknown
[86]	TUB	Yes	Yes, fuel system mass	No/unknown	Yes, fuel system mass

the combustion chamber is anticipated, emphasizing the likelihood of a longer lifetime and fewer required maintenance checks of hydrogen gas turbines. According to [2, p.219] a factor of 0.7 is adopted.

- The larger airframe, advanced propulsion distribution system, and the LH_2 tanks are likely to increase the airframe maintenance cost due to shorter maintenance intervals (see [6, p.27], [27, p.161]). Unfortunately, no relevant data is available. Thus, in [4], a factor range is used, and in [27] the repair costs are scaled with the increased OEM of hydrogen aircraft in addition to a man-hour increase of 7% (arbitrary choice). In this work, the OEM scaling is adopted and the additional increase of man-hours is accounted for in a parameter study in Sect. 3.4.
- Since studies on the turnaround time of LH_2 aircraft showed that no major time differences in comparison to kerosene-fueled aircraft are to be expected [3, 83, 87, 97, 98], the block time and aircraft utilization calculations of the DOC method remain unchanged.

As described above, the TUB DOC model is enhanced with environmental charges, such as noise and NO_x. The NO_x emissions of the LH_2 aircraft are calculated as outlined in Sect. 2.2. Noise emissions are more difficult to estimate, and hence, this work relies on the results of previous LH_2 aircraft studies. The results of the CRYOPLANE study indicate that no change in noise compared to a kerosene-burning aircraft is to be expected [1, p.4]. Steiner reasons that the LH_2 aircraft concept would be quieter than a kerosene-burning aircraft sized for the same requirements because of the lower MTOM, thus either resulting in (1) a shorter take-off runway and higher climb slope for the same thrust, or (2) smaller required engines for a constant design point [27, p.7]. Brewer et al. computed the noise levels of two LH_2 aircraft designs (mid-range and long-range) according to FAR Part 36 (see Table 11) [83].

The main findings of Brewer are that irrespective of design range, LH_2 aircraft are quieter at the flyover point, have similar noise at sideline, and are noisier during the approach. Brewer suggests that the lower noise at flyover can be attributed to the lower MTOM and that the larger noise during approach originates in the fact that the LH_2 aircraft need a higher throttle setting to maintain the 3° glide slope during approach because they have smaller engines and a lower lift-to-drag ratio, but the same mass as the kerosene-counterpart after the full mission. [83, p.185]

Based on these findings, two cases are examined in Sect. 3.4 in a parameter study: (1) no change in noise compared to the kerosene-burning aircraft, and (2) −5EPNdB at flyover, −0EPNdB at sideline, and +1.5 EPNdB at approach compared to the kerosene-burning aircraft.

2.3.3 Summary

To economically assess the different aircraft concepts, the TUB DOC model [72] is considered in this study. Minor enhancements including the environmental charges are included. The model was extended with the options for biofuel and hydrogen aircraft, whereas for biofuel (both BtL and HVO) only the fuel price is changed to an estimated value of 2.6 $€_{2019}$/kg based on an extensive literature review (cf. 0.517 $€_{2019}$/kg for kerosene). For the LH_2 aircraft, changes for the fuel price (2.66 $€_{2019}$/kg), the aircraft price (factor of 1.3), the engine (factor of 0.7) and airframe maintenance costs (factor of 1.07) are incorporated. In terms of the environmental charges, NO_x emissions for A332-H are adapted, but the same noise assumptions as for A332-K are considered.

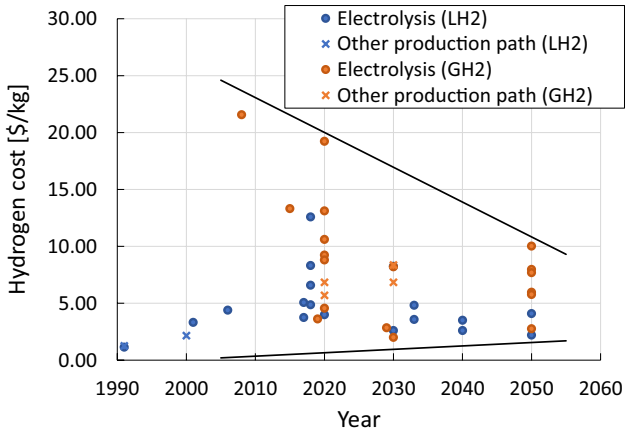

Fig. 9 Hydrogen cost estimations from the literature (data from [2, 3, 6, 27, 83, 86, 88–96]). Note that most studies did not include information about the year the price was attributed to if it was a prediction for the future. If a paper only included a value for an unspecified "future" year, it was assumed that it would be +15years from the study's date of publication

3 Results and discussion

The results of applying the established methodology are presented in this chapter. It is subdivided into five parts: in Sect. 3.1, a comparison of the A332-K and A332-H in terms of aircraft design is presented, in Sects. 3.2 and 3.3, the eLCA and DOC results are shown, and in Sect. 3.4, the parameter studies are discussed. Lastly, in Sect. 3.5, the results are summarized. It should be highlighted that the ecological and economic assessment results have to be interpreted as benchmarks as the high need for assumptions leads to higher uncertainty.

3.1 Design comparison of A332-K and A332-H

The aircraft design of the A332-K and A332-H is undertaken based on the methodology described in Sect. 2.1. The essential specifications are provided in Table 12.

As MTOM decreases (by 16.4%), the wing area and span reduce which is due to the constant aspect ratio (see Table 1) and a similar wing loading, respectively the design point. This ensures that both A332-K and A332-H have comparable take-off and landing field lengths. Additionally, the fuselage length decreases slightly and the diameter increases significantly due to the double deck configuration. As a consequence, the lift-to-drag ratio decreases. Furthermore, the OEM increases by 9.51% due to the heavy hydrogen tanks (6.26 t total, 0.794 gravimetric efficiency), additional reinforcements in wing and fuselage, additional systems mass, and the related snowball effects. Due to these reasons and due to the higher LHV, the fuel mass reduces by 63.3%. The lower mass results in a slight flater cruise slope (mission profile see Appendix Fig. 17; initial cruise altitude fixed see Table 1). Overall, although the fuel mass is drastically reduced, the energy use of the A332-H increases by 2.87%.

To validate the results, the following sources were used: The estimation of the tank mass is comparable to the results of Brewer [2], given that his design has a 6.5% higher fuel mass and that in this study 30% tank weight is saved due to the use of CFRP. For the same design range, similar payload mass, same insulation type, but with different structural improvement factors and aluminum tanks, he estimated a total tank mass of 10.5 t [2, Table 4-38]. The energy use, however, varies widely in the literature. For long-range aircraft, Brewer states a reduction of 12% [2, Table 4-15], but within the report of Airbus an increase by 9% is assumed (based on a minimum change approach) [1]. Troeltsch et al. estimated a 1% reduction when comparing the optimum conventional to the LH_2 design [5]. The result is strongly dependent on the chosen baseline aircraft and their design assumptions, which are often not clearly stated. However, similar results to this study are shown in [29, Fig.2], in which Verstraete determines the variation of energy efficiency with range. With similar TLARs made in this study, Verstraete predicts an energy increase of 5%.

Figure 10 depicts the new design of the hydrogen aircraft in a 3D view.

3.2 eLCA results

Seven configurations were examined in the eLCA: (1) A332-K, (2) A332-H with LH_2 based on steam methane reforming, (3) A332-H with LH_2 produced from electrolysis, (4) A332-BF with BtL produced with the current EU electricity mix, (5) A332-BF with BtL produced with renewable energies, (6) A332-BF with HVO produced with the current EU electricity mix, (7) A332-BF with HVO produced with

Table 11 Noise levels in [EPNdB] of FAR Part 36 noise analysis of transport aircraft from [83, Tab. 33]

	Mid-range			Long-range		
[EPNdB]	Jet A	LH_2	Δ	Jet A	LH_2	Δ
Flyover	92.68	88.11	−4.57	94.23	89.20	−5.03
Sideline	86.40	86.38	−0.02	87.80	87.16	−0.64
Approach	96.63	97.86	+1.23	96.70	98.44	+1.74

renewable energies. These concepts were finally evaluated based on the environmental impact indicator *single score* to investigate whether and to what extent the environmental impact can be reduced in comparison to the kerosene-powered aircraft. Table 16 in Appendix 2 summarizes the absolute single score values for all aircraft concepts for the baseline scenario (steam reforming or EU-mix of electricity) and future scenario (electrolysis or renewable energies).

Figure 11 shows the relative SS change of A332-H and A332-BF compared to the A332-K in both scenarios (baseline in filled, future in patterned bars).

For all configurations in the baseline scenario, the total SS is higher compared to the reference (A332-BF (BtL): +548%, A332-BF (HVO): +238%, A332-H: +14.8%), which means that these configurations are more harmful than the A332-K. For the H_2 aircraft, this is mainly linked to (1) CO_2 emissions in the H_2 process of steam reforming and (2) the formation of contrails and cirrus clouds due to the combustion of hydrogen. These effects result in increased damage to human health (+37.2%) and ecosystem diversity (+39.1%) leveling out the positive effect of the decreased damage on resource availability (−47.1%). For both biofuels, all endpoint categories are negatively affected due to the high energy demand in the fuel production process that compensates the beneficial effect of algae of being capable of binding CO_2 during its cultivation. However, HVO has a lower impact because the process requires half as much energy as the BtL process.

For all configurations in the future scenario, the total SS is lower compared to the reference, which means that they are less harmful than the A332-K (A332-BF (BtL): −35.8%, A332-BF (HVO): −112%, A332-H: −59.5%). The major driver for A332-BF (BtL) and A332-H is the lower damage to resource availability (−73.7%, −99.0% respectively). Their production processes require less mineral or fossil fuel resources such as crude oil or natural gas. Additionally, switching to electrolysis and renewable energies drastically reduces CO_2 emissions. The highest impact reduction is achieved by A332-BF (HVO). The reason lies in Johanning's methodology, in which the input and outputs for the production of 1 kg HVO biofuel with renewables only require CO_2 (other fall below the cut-off criterion, see Table 5). These findings match the tendencies of the results of Johanning [22, 55].

3.3 DOC results

In the DOC analysis, three configurations were examined in the EIS year 2040: (1) A332-K, (2) A332-H, and (3) A332-BF (because no differentiation was made between the two biofuel production processes, see Sect. 2.3.1).

Table 12 Key specifications of the A332-H compared to the reference aircraft A332-K (EIS 2040)

	A332-K	A332-H	Δ
Wing area (m^2)	312	262	−16.0%
Wing span (m)	56.1	51.3	−8.56%
Fuselage length (m)	57.9	57.7	−0.35%
Fuselage diameter (m)	5.70	7.25	+27.2%
MTOM (kg)	198, 500	165, 900	−16.4%
OEM (kg)	94, 050	103, 000	+9.51%
Fuel mass[a] (kg)	65, 530	24, 040	−63.3%
Lift-to-drag ratio (–)	21.3	20.0	−6.10%
Energy use (kJ/100km/seat)[b]	9.40	9.67	+2.87%

[a]Block and reserves

[b]LHV kerosene 42.8 MJ/kg, H_2 120 MJ/kg

Figure 12 compares the shares of the DOC elements (capital, energy costs etc.) of A332-K, A332-H and A332-BF relative to the total DOC of the conventional aircraft.

It shows two important outcomes: First, the highest cost share for all configurations is the energy cost (A332-K: 0.52, A332-H: 0.54, A332-BF: 1.60), whereas the lowest share has the environmental fee (A332-K: 0.01, A332-H: 0.00, A332-BF: 0.01). Secondly, both the hydrogen and the biofuel aircraft show an increase in total DOC (A332-H: +10.8%, A332-BF: +108%). For the hydrogen aircraft, this is linked to its higher OEM and H_2 cost and therefore increased capital and energy cost. For the biofuel aircraft, it is attributed to the high fuel cost. The results for the conventional aircraft can be validated based on the study of Lee et al. which analyzes the DOC of wide-body passenger aircraft in Hong Kong [99, Figure 9]. The estimate of 10 cent / (NM-PAX) for the A330-200 operating in long-haul mode with 300 passengers approximates the results of this study at 9 cent /(NM-PAX).

3.4 Parameter studies

As discussed in Chapter 2, there are inputs in the design, the eLCA, and the DOC model that underlie uncertainties (e.g. the in-flight boil-off, contrail radiative forcing, and the fuel price). To analyze the potential impact on the results, parameter studies for these values were conducted. In Sect. 3.4.1, results of the parameter studies that have a major impact on the aircraft design, the eLCA, or DOC results are shown. Results with a minor impact are described in Sect. 3.4.2.

3.4.1 Parameters with major impact

The first parameter study with a major impact shown in Fig. 13 deals with a design variation and depicts the effect

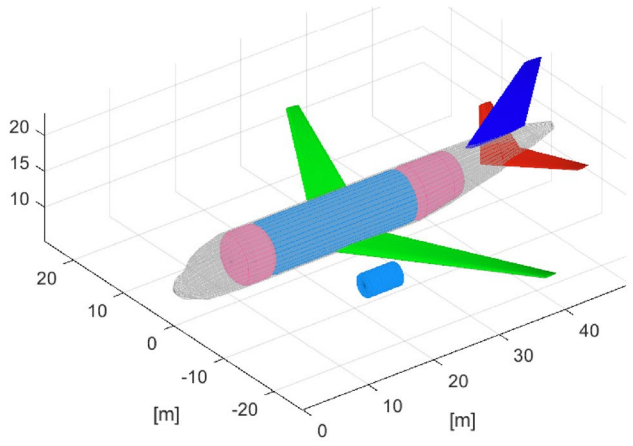

Fig. 10 3D views of A332-H in ADEBO (cabin in light blue, tanks in pink)

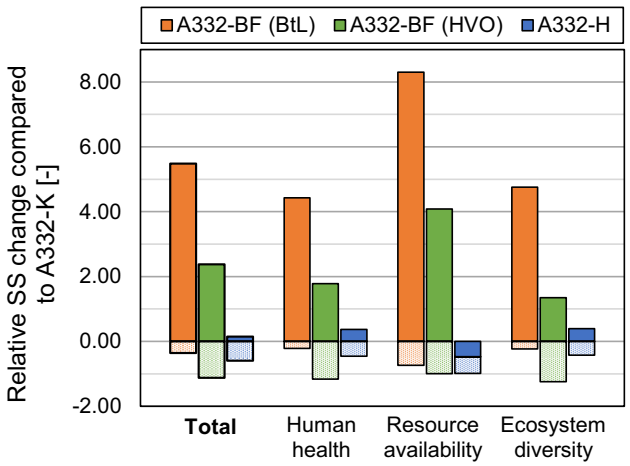

Fig. 11 Relative SS change of A332-BF and A332-H compared to A332-K in baseline (filled) and future (dotted pattern) scenario

of the hydrogen tank material (CFRP and aluminum), shape and position (conic in tail and cylindrical in cabin) on the A332-H specifications.

The figure shows the negative impact for both (1) a conic aluminum tank and (2) a cylindrical CFRP aft tank. The first case has, as expected, a large effect on OEM due to the heavy tanks (8.79 t instead of 6.26 t). The fuselage length is slightly increased by 0.16% due to the increased fuel mass (2.08%). The second case has a greater effect due to the increased fuselage length by 8.99% which results in an increased fuel mass (5.42%) and a reduced lift-to-drag ratio (1.20%). Overall, both configurations result in a MTOM increase of 2.87 and 3.34%, respectively.

Another design parameter variation deals with the effect of tank mass or gravimetric tank efficiency $\eta_{grav,tank}$ on the A332-H design. As mentioned in Sect. 2.1.3.3, a range of 0.3 to 0.85 for $\eta_{grav,tank}$ is feasible, whereas the 0.793 in the baseline case is in the upper and more optimistic range. To investigate the lower and pessimistic range, factors of 6 and 7 were applied on the tank mass in the design process. This results in $\eta_{grav,tank}$ of 0.390 and 0.353 and yields a similar result shown in the Clean Sky report [6] (0.380 efficiency, +42.0% energy use). In Fig. 14, the A332-H changes with different $\eta_{grav,tank}$ compared to the A332-K are displayed (including [6] case): it is visible that $\eta_{grav,tank}$ and respectively the tank mass has a significant impact on the aircraft design in this study increasing the energy demand from +2.87% for the baseline A332-H to +35.6% or +40.8% for a more pessimistic view.

After discussing design parameter studies, in the following two parameter variation concerning eLCA are presented.

The first eLCA parameter study was conducted for the $EINO_x$ configurations for the A332-H. If the injector configuration C4 (cruise $EINO_x = 0.63$) is selected instead of C3 (cruise $EINO_x = 3.14$), the total SS reduces in the baseline scenario by 1.23% and in the future scenario by 2.69%. Comparing these results with the effects of contrail radiative forcing mentioned next, the reduction from the contrails radiative forcing has a higher impact. This is supported by the studies of [63], which attribute a higher effective radiative forcing to contrails and cirrus clouds than to NO_x emissions (57.4 and 17.5 m W/m^2, respectively).

The next parameter variation concerns the reduction of the contrail radiative forcing which affects the eLCA of A332-H and A332-BF BtL and HVO. Fig. 15 shows the behavior on the relative SS compared to the A332-K by varying the contrail radiative forcing factor for both baseline and future scenario. As discussed in Sects. 2.2.1 and 2.2.2, the base reduction factor for the contrail radiative forcing is set to 0.4. The figure shows that by increasing the reduction factor the relative SS linearly reduces and vice versa, e.g. for the A332-BF (BtL) in the baseline scenario, the SS is +548% for a 0.4 factor, reduced to +544% for a 0.6 factor, and increased +553% for a 0.2 factor. For all biofuel configurations, a gradient of 2.10% per 0.1 variation of the contrail radiative forcing is visible. The H_2 configurations are more sensitive with a gradient of 5.58% per 0.1 factor variation.

Next, the economical aspects are considered. Given that it is currently unknown what the capital cost impact of a transition to a H_2 aircraft would be, a parametric study was conducted in this context. The baseline factor of 1.3 is examined and varied by −100 to +100% (see Fig. 19 in the Appendix 4). The results show, that per 10% increase in the factor, the capital cost increases by 14.7% and the total DOC by 3.2%. If instead of a factor of 1.3, a factor of 0.88 was chosen, the capital costs of the A332-H would be similar to that of the A332-K. This is because the capital cost derivation also includes the OEM. It can be concluded, that the factor has a

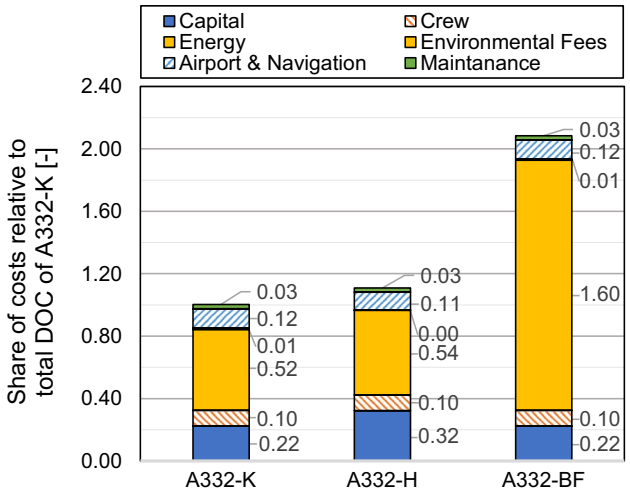

Fig. 12 Comparison of DOC shares of A332-K, A332-H, and A332-BF (same for BtL and HVO) in EIS year 2040

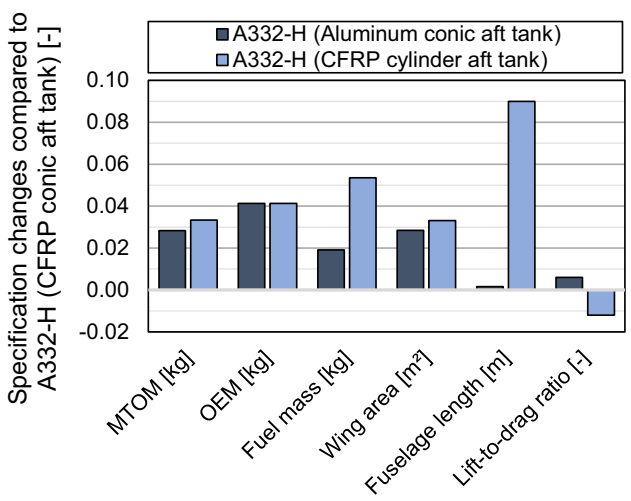

Fig. 13 Parameter study of the effect of tank shape and material on A332-H specifications

decisive effect on the total DOC, but is not a realistic factor in leveling the costs between the A332-K and A332-H.

Another parameter study considered is the fuel price escalation of kerosene (baseline 2%, see Table 9). To assess the sensitivity, a variation from 0 to 4% was conducted in this context. The results show that doubling the escalator will lead to 26% higher total cost per flight—halving it will decrease it by 10% (see Appendix Fig. 20). Even though the total cost per flight is highly sensitive to the jet fuel price escalator, there are few forecasts for its prediction. For crude oil, the Annual Energy Outlook 2022 expects growth of 3.1% p.a. from 2021 to 2050 (Brent crude oil spot prices [100]). However, previous statistics showed that the price of jet fuel is highly dependent on world occurrences. Events like the European debt crisis, the fracking boom, the COVID-19 pandemic, and the Ukraine war had all an impact on forecasting the price (e.g., [101]).

Additionally, the LH_2 and biofuel price influence on DOC are examined in a parameter study. Fig. 16 shows the relative change in total DOC of the A332-H and A332-BF compared to the A332-K plotted against the change in fuel price.

There are two important findings: firstly, the fuel price is a decisive factor in the total DOC because of its high proportion of the energy cost (compare Fig. 12). Per 10% increase in the hydrogen fuel price, the total DOC increases by 5.43%, while for the aircraft utilizing biofuels an increase of 16.0% results. Secondly, the hydrogen fuel price needs to fall by 23.9% and the biofuel price by 67.5% respectively, to achieve the same conventional aircraft total DOC. One proposal to reduce the hydrogen fuel cost is to use potential synergy effects at the airport and hence to increase economics of scale. This is illustrated in Fig. 18 in the Appendix, which shows the options for the LH_2 supply and use

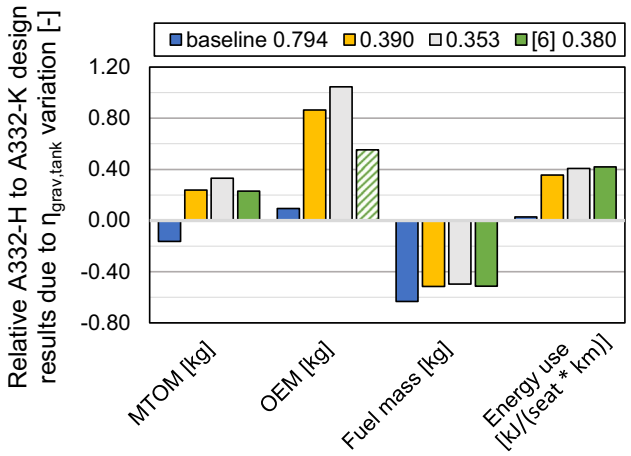

Fig. 14 Parameter study of gravimetric tank efficiency $\eta_{grav,tank}$ (baseline 0.794) reduction effect on A332-H (OEM of [6] is calculated based on the assumption of an 52 t increase due to the tanks)

at airports. To increase the economies of scale, hydrogen-powered land-side traffic (cars, cabs, shuttles, buses) and ground support vehicles are particularly useful in increasing the economies of scale. Likewise, it can be envisioned that LH_2 is also resold locally by the airport.

3.4.2 Parameters with Minor Impact

The following describes the results of parameter studies that have a minor impact (< 0.5%) on their evaluation criterion: The examined in-flight boil-off has a minor effect on the MTOM, OEM, and necessary fuel mass of the A332-H design (Fig.21 in Appendix 4). The results show that the impact of a 10% change in the venting percentage has an impact of 0.2% on the fuel mass and energy

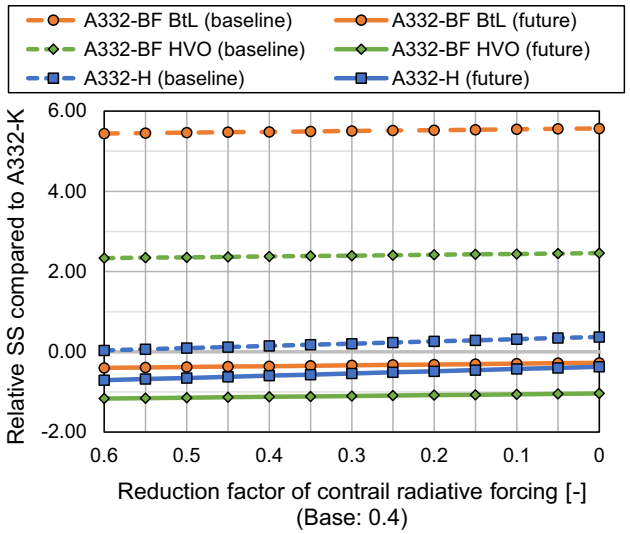

Fig. 15 Parameter study of contrail radiative forcing reduction effect on A332-H and A332-BF compared to A332-K

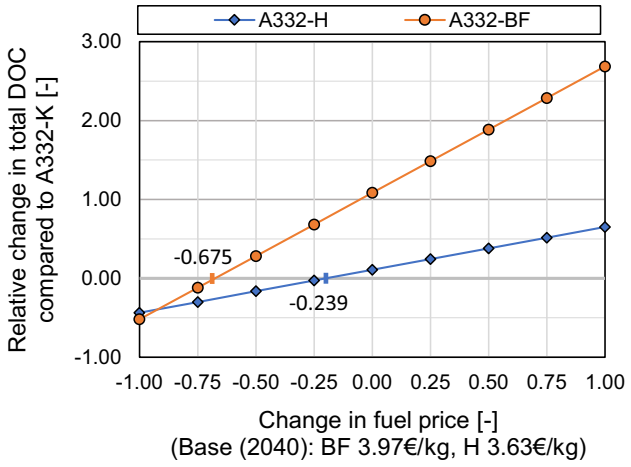

Fig. 16 Parameter study of fuel price effect on the total DOC of A332-H and A332-BF referenced to A332-K

efficiency. Parameter studies which have a minor effect on the total DOC are the change in the man-hour factor, the noise cases, and the $EINO_x$ configurations. The results show that the impact of a 10% change in the man-hours factor has an impact of 0.1% on the total DOC (see Fig. 22 in Appendix 4). Comparing the two noise cases presented in Sect. 2.3.2, the results show an impact of 0.01% on the total DOC. This is because the noise and emissions costs have a total DOC share of < 0.1%. Comparing configurations C3 and C4 for the $EINO_x$, the results show an impact of −0.1% on the total DOC. This is due to the abovementioned correlation of a low emissions cost share. Due to the minor influence on the overall results, the assumed values are considered acceptable.

3.5 Summary

Table 13 gives an overview of the results conducted in Sects. 3.1–3.3 and of the parameter studies in Sect. 3.4.

4 Conclusion and future work

This study has developed a methodology to design and evaluate long-range hydrogen and biofuel transport aircraft with respect to their environmental life cycle and direct operating cost. Different scenarios have been investigated and parameter studies conducted, thus determining under which conditions hydrogen and biofuel aircraft might be a viable option for reducing aviation's climate impact. The main findings of the study are that (1) in terms of the aircraft design, liquid hydrogen as a fuel offers a significant reduction in fuel mass, but increases energy consumption, (2) for both biofuel and hydrogen aircraft the highest priority is covering energy demand with renewable energies to reduce the climate impact, and (3) both new propellants result in higher operating costs than conventional aircraft. The main drivers of this study that would achieve an environmental impact reduction and lower operating costs are lightweight hydrogen storage tanks, reduced contrail radiative forcing, and low hydrogen and biofuel prices. Table 14 summarizes the main findings of this study in respect of the environmental (SS) and economic (DOC) evaluation of hydrogen and biofuel aircraft.

Hence, it can be concluded that the use of hydrogen or biofuel as propellants offers a potential solution for achieving the objective of an environmentally neutral aviation industry. Here, it should be considered whether the effort involved in a new aircraft design required for the use of hydrogen compared to the use of drop-in biofuels is worthwhile, in particular when biofuels such as HVO are considered. This strongly depends on the results of contrail radiative forcing research and the political fuel price subsidy and taxation decisions made for both propellants.

An important paradox should also be highlighted here, as the results of the paper contradict current politics. The current trend to use SAFs as a way to combat climate change should be taken with caution. Despite the ease of implementation in the aircraft due to the possible 100% replacement of kerosene, huge drawbacks can result due to the energy demand of the fuel production process. A hydrogen-powered aircraft also seems to be a solution, although its development and construction is still in its infancy. It should also be emphasized that the lack of mission range flexibility can be a serious problem and may prevent fleet integration and use by airlines.

Table 13 Overview of the design, eLCA, and DOC studies and results

	General	Major impact parameter study	Minor impact parameter study
Design	A332-K (BF as drop-in) and A332-H: results in Table 12	(1) H_2 tank material (CFRP/ alu) & location (tail/ cabin) (2) $\eta_{grav,tank}$	(1) H_2 in-flight boil-off
eLCA	7 configurations: results in Fig. 11	(1) H_2 injection configuration (2) H_2 & BF contrail radiative forcing	
DOC	3 configurations: results in Fig. 12	(1) H_2 capital cost impact (2) Kerosene fuel price escalation (3) H_2 & BF fuel price	(1) H_2 man-hour factor (2) H_2 noise (3) H_2 injection configuration

Table 14 Relative comparison of SS and DOC of A332-H and A332-BF versus A332-K

		Baseline scenario	Future scenario
eLCA	A332-H	+14.8%	−59.5%
	A332-BF (BtL)	+548%	−35.8%
	A332-BF (HVO)	+238%	−112%
DOC	A332-H	+10.8%	
	A332-BF	+108%	

Future work associated with this study should consider improvements to the hydrogen and biofuel design processes with more detailed models and adaptions. Topics that could be further exploited in order to increase the accuracy of the hydrogen design, are the wing surface cooling for laminar flow [2, 102] and the engine TSFC increase [2, 103]. The biofuel aircraft design process can be adapted to take into consideration its higher LHV and lower density. Furthermore, investigations of the integration of hydrogen-powered fuel cells or other SAFs based on e.g. cooking oil would be of interest.

Additionally, H_2 safety standards are still open in discussion which can influence essential assumptions in this design, such as the front-and-aft storage tank configuration. Also, the impact of off-design missions on hydrogen aircraft should be considered in detail. The inflexible operations in range of this aircraft concept could lead to an impact on air transport systems such as the fleet or network modeling.

Of equal importance is using an up-to-date database to reflect the latest developments in eLCA and updating the model to the fully revised ReCiPe 2016 methodology.

A Appendix

A.1 NO_x Emission index derivation and input data

Derivation of *ppmNOx* to EI_{NO_x} conversion:

$$
\begin{aligned}
EI_{NO_x}\left[\frac{g_{NO_x}}{kg_{H_2}}\right] &= \frac{\dot{m}_{NO_x}}{\dot{m}_{\text{fuel}}}\cdot\frac{10^3\ g}{\text{kg}} \\
&= \frac{\dot{m}_{NO_x}}{\dot{m}_{air}\cdot FA_{H_2}}\cdot\frac{10^3\ g}{\text{kg}} \\
&= \frac{\dot{m}_{NO_x}}{\dot{m}_{air}\cdot FA_{H_2}}\frac{\dot{m}_{\text{air}}\,(1+FA_{H_2})}{\dot{m}_{\text{exhaust}}}\cdot\frac{10^3\ g}{\text{kg}} \\
&= \frac{1+FA_{H_2}}{FA_{H_2}}\frac{\dot{m}_{NO_x}}{\dot{m}_{\text{exhaust}}}\cdot\frac{10^3\ g}{\text{kg}} \\
&= \frac{1+FA_{H_2}}{FA_{H_2}}\frac{m_{NO_x}}{m_{\text{exhaust}}}\cdot\frac{10^3\ g}{\text{kg}}
\end{aligned}
\tag{8}
$$

Assume that $NO_x \approx NO_2$, with molar mass $M_{NO_2} = 46$ g/mol. From stoichiometric combustion of hydrogen with air, the molar mass of the exhaust $M_{exhaust}$ is found:

$$
H_2 + 0.5(O_2 + 3.76N_2) \longrightarrow 1H_2O + 1.88N_2 \tag{9}
$$

$$
\begin{aligned}
M_{\text{exhaust}} &= \frac{1}{1+1.88}\cdot M_{H_2O} + \frac{1.88}{1+1.88}\cdot M_{N_2} \\
&= \frac{1}{1+1.88}\cdot 18\ \text{g/mol} + \frac{1.88}{1+1.88}\cdot 28\ \text{g/mol} \\
&\approx 24.5\ \text{g/mol}
\end{aligned}
\tag{10}
$$

Then with $m = M \cdot n$:

Table 15 Inputs for EI_{NO_x} calculation for C3 and C4 (Equations 4, 5, 6)

Input	Value
P_3	1.257MPa
ϕ_{H_2}	$FA_{H_2}/0.0292 = 0.02103$
τ	2 ms
T_3	735 K
FA_{H_2}	fuel flow/core flow = $FA_{\text{Kero}}/2.55 = 0.9527/2.55$ $/(444.882/(1+6.3077)) = 0.00614$

For cruise conditions, P_3, T_3, FA_{H_2} and τ were estimated from the data of a Trent 892 turbofan as provided in [104]

$$EI_{NO_x}\left[\frac{g_{NO_x}}{kg_{H_2}}\right] = \frac{1+FA_{H_2}}{FA_{H_2}}\frac{n_{NO_2}\cdot 46\ \text{g/mol}}{n_{\text{exhaust}}\cdot 24.5\ \text{g/mol}}\cdot\frac{10^3\ g}{\text{kg}} = \frac{1+FA_{H_2}}{FA_{H_2}\cdot 533}\cdot ppmNOx \tag{11}$$

A.2 eLCA results supplementary information

See Table 16.

Table 16 Comparison of total SS [points/passenger-kilometer] of hydrogen and biofuel fueled versus conventional aircraft for the baseline and future scenario

	A332-K	A332-H	A332-BF (BtL)	A332-BF (HVO)
Baseline	1.42E−02	1.63E−02	9.20E−03	4.79E−02
Future	–	5.74E−03	9.11E−03	− 1.73E−03

A.3. Mission profile

See Fig. 17.

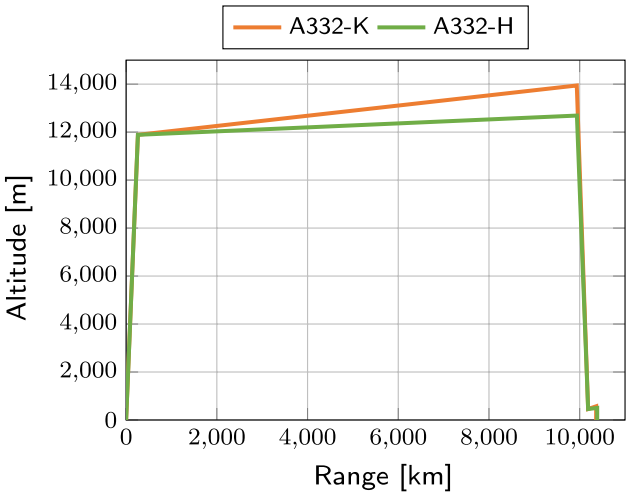

Fig. 17 Mission profiles of A332-K and A332-H

A.4 Parameter study results

See Figs. 18, 19, 20, 21 and 22.

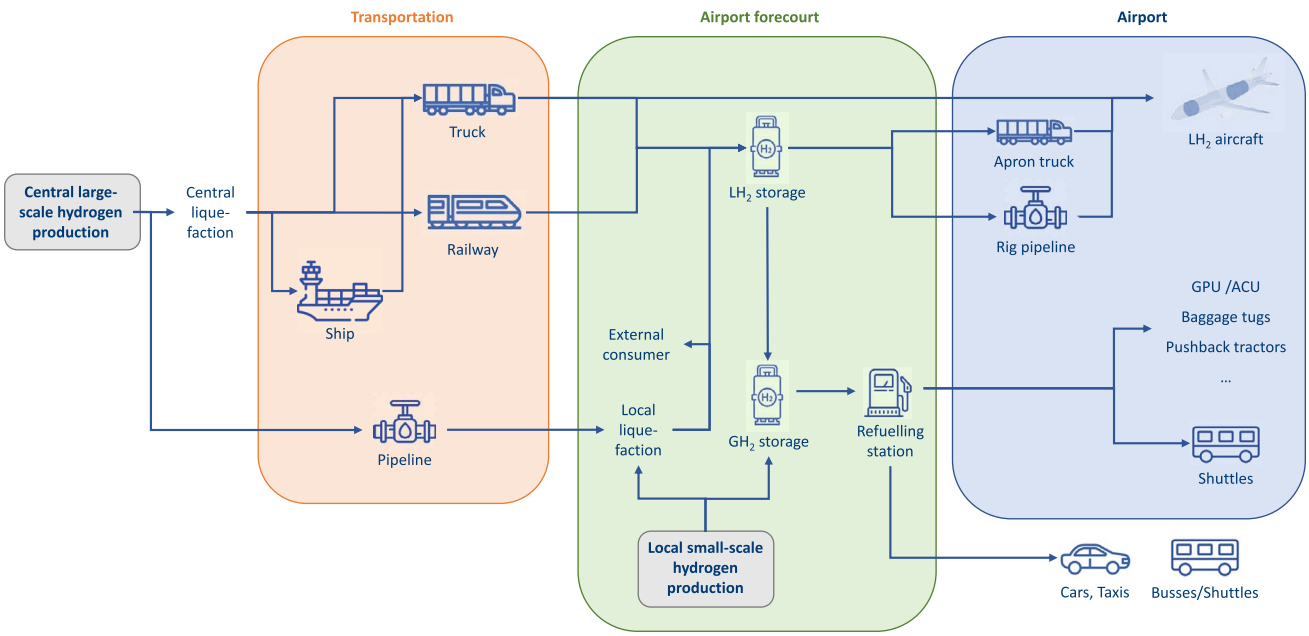

Fig. 18 Options for LH_2-supply of airports and its usage (from [105, Fig. 2])

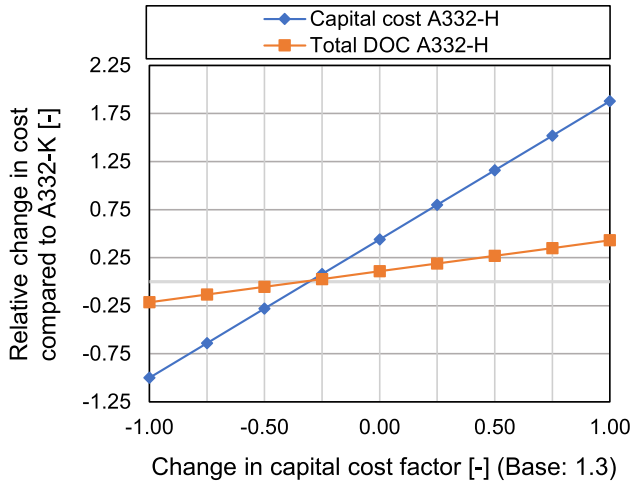

Fig. 19 Capital cost factor for A332-H

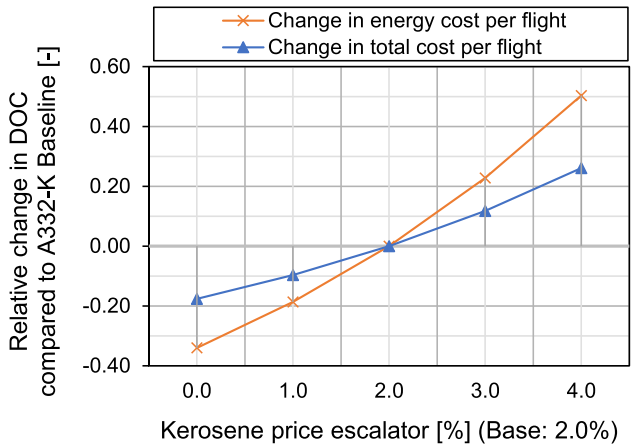

Fig. 20 Kerosene price escalator for A332-K

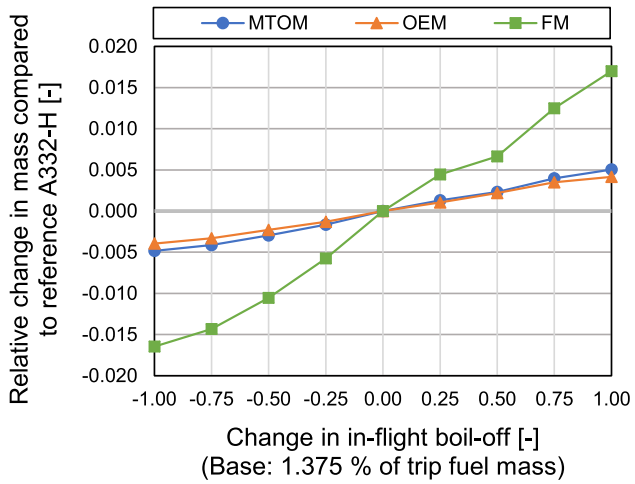

Fig. 21 Effect of in-flight boil-off on the masses of A332-H

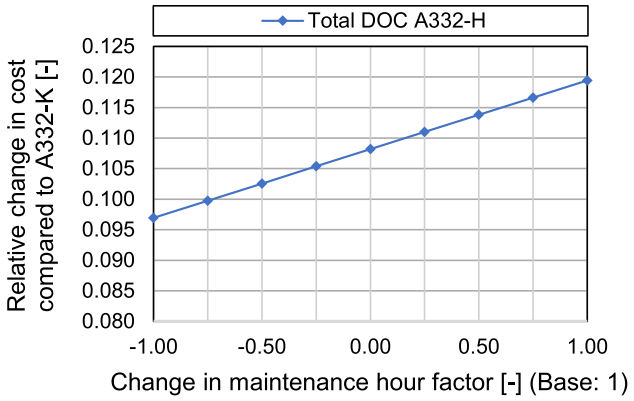

Fig. 22 Maintenance hour factor for A332-H

Funding Open Access funding enabled and organized by Projekt DEAL. Funding by Technical University of Munich.

Declarations

Conflict of interest The authors declare that they have no conflict of interest.

Code availability Custom code.

References

1. Airbus: Liquid hydrogen fuelled aircraft—system analysis. Tech. Rep. GRD1-1999-10014, Airbus Deutschland GmbH (2003)
2. Brewer, G.D.: Hydrogen aircraft technology. CRC Press Inc, Boca Raton (1991)
3. Sefain, M.J.: Hydrogen aircraft concepts & ground support. Ph.D. thesis, Cranfield University, Cranfield, United Kingdom (2000)
4. Verstraete, D.: The potential of liquid hydrogen for long range aircraft propulsion. Ph.D. thesis, Cranfield University, Cranfield, United Kingdom (2009)
5. Troeltsch, F., Engelmann, M., Peter, F., Kaiser, J., Hornung, M., Scholz, A.E.: Hydrogen powered long haul aircraft with minimized climate impact, in Proc AIAA AVIATION 2020 FORUM. AIAA Aviation Forum, Virtual Event (2020)
6. McKinsey & Company: Hydrogen-powered aviation: A fact-based study of hydrogen technology, economics, and climate impact by 2050. Tech. rep., McKinsey & Company (2020)

7. IATA: Developing sustainable aviation fuel (SAF) (2021). https://www.iata.org/en/programs/environment/sustainable-aviation-fuels/. Accessed 07 June 2021
8. Herbst, S.: Development of an aircraft design environment using an object-oriented data model in matlab. Ph.D. thesis, Technical University of Munich, Munich, Germany (2018)
9. Roskam, J.: Airplane design. DARcorporation, Lawrence, Kansas (1986)
10. Jenkinson, L., Simpkin, P., Rhodes, D.: Civil jet aircraft design—aircraft data file A330-200 (2001). https://booksite.elsevier.com/9780340741528/appendices/data-a/table-1/table.htm. Accessed 14 June 2021
11. Airbus: A330 aircraft characteristics—airport and maintenance planning (2020). Issue: Jan 01/93, Rev: Jun 01/20
12. Schmitt, D., Gollnick, V.: Air transport system. Springer Verlag, Vienna (2016)
13. Eurocontrol: Base of aircraft data (BADA) of A330-200 (2009). APF file, Creation date: May 22 2003, Modification date: Mar 05 2009
14. Roux, E.: Turbofan and turbojet engines—database handbook. Editions Elodie Roux, Blagnac (2007)
15. ACI Airports Council International: ACI aircraft noise rating index (2010)
16. Berdowski, Z., van den Broek-Serlé, F.N., Jetten, J.T., Kawabata, Y., Schoemaker, J.T., Versteegh, R.: Survey on standard weights of passengers and baggage (2009)
17. Office of the Federal Register: Electronic code of federal regulations (eCFR) (2021). 14 C.F.R §121.391, https://www.ecfr.gov/. Accessed 14 June 2021
18. Verstraete, D.: Long range transport aircraft using hydrogen fuel. Int. J. Hydrogen Energy **38**(34), 14824 (2013). https://doi.org/10.1016/j.ijhydene.2013.09.021
19. Blakey, S., Rye, L., Wilson, C.W.: Aviation gas turbine alternative fuels: a review. Proc. Combust. Inst. **33**(2), 2863 (2011). https://doi.org/10.1016/j.proci.2010.09.011
20. Rahmes, T., Kinder, J., Crenfeldt, G., LeDuc, G., Abe, Y., McCall, M., Henry, T., Zombanakis, G., Lambert, D., Lewis, C., Andac, M., Juenger, J., Reilly, K., Holmgren, J., Bozzano, A.: Sustainable bio-derived synthetic paraffinic kerosene (bio-spk) jet fuel flights and engine tests program results, in Proc 9th AIAA Aviation Technology, Integration, and Operations Conference. AIAA Aviation Forum, Hilton Head (2009)
21. International, A.: Astm d1655-20d—standard specification for aviation turbine fuels (2020)
22. Johanning, A.: A method for the environmental life cycle analysis during conceptual aircraft design [methodik zur ökobilanzierung im flugzeugvorentwurf]. Ph.D. thesis, Technical University of Munich, Munich, Germany (2017)
23. Anisha, G., John, R.: 9—Bio-engineering algae as a source of hydrogen. In: Basile, A., Iulianelli, A. (eds) Advances in Hydrogen Production, Storage and Distribution, pp. 248–262. Woodhead Publishing (2014). https://doi.org/10.1533/9780857097736.2.248
24. Godula-Jopek, A., Westenberger, A.: Hydrogen-fueled aeroplanes, in Compendium of Hydrogen Energy (2016)
25. Colozza, A., Kohout, L.: Hydrogen storage for aircraft applications overview. Tech. Rep. NASA CR–2002-211867, Analex Coperation, Hampton, Virginia, United States (2002)
26. Chen, Z., Li, P., Anderson, R., Wang, X., Zhang, X., Robison, L., Redfern, L.R., Moribe, S., Islamoglu, T., Gómez-Gualdrón, D.A., Yildirim, T., Stoddart, J.F., Farha, O.K.: Balancing volumetric and gravimetric uptake in highly porous materials for clean energy. Science **368**, 297 (2020). https://doi.org/10.1126/science.aaz8881
27. Steiner, J.: Minimal change retrofit of a wide-body transport aircraft für operation with liquid hydrogen [umrüstung eines großraumverkehrsflugzeuges für den betrieb mit flüssigem wasserstoff unter vermeidung konfigurativer änderungen]. Master's thesis, Technical University of Berlin, Berlin, Germany (2001)
28. Khandelwal, B., Karakurt, A., Sekaran, P.R., Sethi, V., Singh, R.: Hydrogen powered aircraft: the future of air transport. Prog. Aerosp. Sci. **60**, 45 (2013). https://doi.org/10.1016/j.paerosci.2012.12.002
29. Verstraete, D.: On the energy efficiency of hydrogen-fuelled transport aircraft. Int. J. Hydrogen Energy **40**(23), 7388 (2015). https://doi.org/10.1016/j.ijhydene.2015.04.055
30. Scholz, D., Dib, L.: Hydrogen as future fuel used in minimum change derivatives of the airbus a321 (2015). [Presentation] Deutscher Luft- und Raumfahrtkongress 2015, Rostock, Germany. http://www.fzt.haw-hamburg.de/pers/Scholz/Airport2030/Airport2030_PRE_DLRK2015_HydrogenA320_2015-09-22.pdf. Accessed 16 July 2021
31. Winnefeld, C., Kadyk, T., Bensmann, B., Krewer, U., Hanke-Rauschenbach, R.: Modelling and designing cryogenic hydrogen tanks for future aircraft applications. Energies **11**(1), 105 (2018). https://doi.org/10.3390/en11010105
32. Züttel, A.: Hydrogen storage methods. Naturwissenschaften **91**, 157–172 (2004). https://doi.org/10.1007/s00114-004-0516-x
33. Kossarev, K.: Extension of an aircraft design environment for the design and life cycle assessment of a long range hydrogen aircraft. Master's thesis, Technical University of Munich, Munich, Germany (2020)
34. Mital, S., Gyekenyesi, J., Arnold, S., Sullivan, R., Manderscheid, J., Murthy, P.: Review of current state of the art and key design issues with potential solutions for liquid hydrogen cryogenic storage tank structures for aircraft applications. Tech. Rep. NASA/TM–2006-214346, The University of Toledo, N &R Engineering and Glenn Research Center, Toledo and Cleveland, Ohio, United States (2006)
35. Johnson, T.F., Sleight, D.W., & Martin, R.A.: Structures and design phase I summary for the nasa composite cryotank technology demonstration project. Tech. rep., NASA Langley Research Center, Hampton, Virginia, United States (2013)
36. Schultheiß, D.: Permeation barrier for lightweight liquid hydrogen tanks. Ph.D. thesis, University Augsburg, Augsburg, Germany (2007)
37. Verstraete, D., Hendrick, P., Pilidis, P., Ramsden, K.: Hydrogen fuel tanks for subsonic transport aircraft. Int. J. Hydrogen Energy **35**(20), 11085 (2010). https://doi.org/10.1016/j.ijhydene.2010.06.060
38. Timmerhaus, K.D., Flynn, T.M.: Cryogenic process engineering (Springer, US, Boston). Massachusetts (1989). https://doi.org/10.1007/978-1-4684-8756-5
39. Deutsches Institut für Normung e.V.: DIN 28011 torispherical heads (2012)
40. Swiss-composite: Faserverbund werkstoffdaten (2020). https://www.swiss-composite.ch/pdf/i-Werkstoffdaten.pdf. Accessed 14 Oct 2020
41. Grenoble, R.: Mechanical properties and durability of a composite material at cryogenic temperatures. Ph.D. thesis, Old Dominion University, Norfolk, Virginia (2006). https://doi.org/10.25777/ja61-xh69
42. Cytec: Cycom 977-2 epoxy resin system—technical data sheet (2012). https://www.e-aircraftsupply.com/MSDS/104927CYCOM%20977-2%20tds.pdf. Accessed 14 Oct 2020
43. Huete, J., Nalianda, D., Pilidis, P.: Impact of tank gravimetric efficiency on propulsion system integration for a first-generation hydrogen civil airliner. Aeronaut. J. (2022). https://doi.org/10.1017/aer.2022.60
44. Jenkinson, L.R., Simpkin, P., Rhodes, D.: Civil jet aircraft design. Arnold, London (1999)

45. Schäfer, K.: Conceptual aircraft design for sustainability. Ph.D. thesis, RWTH Aachen University, Aachen, Germany (2018)
46. Lopes, J.: Life cycle assessment of the airbus a330-200 aircraft. Master's thesis, Universidade Técnica de Lisboa, Lisbon, Portugal (2010)
47. Howe, S., Kolios, A.J., Brennan, F.P.: Environmental life cycle assessment of commercial passenger jet airliners. Transp. Res. Part D: Transp. Environ. **19**, 34 (2013). https://doi.org/10.1016/j.trd.2012.12.004
48. Chester, M.V.: Life-cycle environmental inventory of passenger transportation in the united states. Ph.D. thesis, University of California, Berkeley, Berkeley, California, United States (2008)
49. Scholz, A.E., Trifonov, D., Hornung, M.: Environmental life cycle assessment and operating cost analysis of a conceptual battery hybrid-electric transport aircraft. CEAS Aeronaut. J. **13**, 215 (2022). https://doi.org/10.1007/s13272-021-00556-0
50. Köhler, M.O., Rädel, G., Dessens, O., Shine, K., Rogers, H., Wild, O., Pyle, J.: Impact of perturbations to nitrogen oxide emissions from global aviation. J. Geophys. Res. Atmos. **113**, D11 (2008)
51. Rädel, G., Shine, K.P.: Radiative forcing by persistent contrails and its dependence on cruise altitudes. J. Geophys. Res. Atmos. **113**, D7 (2008). https://doi.org/10.1029/2007JD009117
52. Goedkoop, M., Heijungs, R., Huijbregts, M., De Schryver, A., Struijs, J., Van Zelm, R.: Recipe 2008: A life cycle impact assessment method which comprises harmonised category indicators at the midpoint and the endpoint level. report i: Characterisation. Tech. rep., Ministerie van Volkshuisvesting, Ruimtelijke Ordening en Milieubeheer (2009)
53. Airbus: Orders and deliveries—commercial aircraft (2020). https://www.airbus.com/aircraft/market/orders-deliveries.html. Accessed 19 July 2021
54. Eurocontrol: standard inputs for eurocontrol cost-benefit analyses (2018). Publication Reference: 17/09/27/149. https://www.eurocontrol.int/publication/standard-inputs-eurocontrol-cost-benefit-analyses-edition-8. Accessed 19 July 2021
55. Johanning, A., Scholz, D.: Comparison of the potential environmental impact improvements of future aircraft concepts using life cycle assessment, in Proc 5th CEAS Air & Space Conference (Council of European Aerospace Societies (CEAS), "Delft, The Netherlands", 2015)
56. Gehrer, M., Seyfried, H., Staudacher, S.: Life cycle assessment of btl as compared to hvo paths in alternative aviation fuel production, in Proc 63rd Deutscher Luft- und Raumfahrtkongress. Deutsche Gesellschaft für Luft-und Raumfahrt (DGLR), Augsburg, Germany (2014)
57. Kalnes, T.N., Marker, T., Shonnard, D., Koers, K.P.: Green diesel production by hydrorefining renewable feedstocks. Biofuels Technol. **4**, 7 (2008)
58. Braun-Unkhoff, M., Riedel, U., Wahl, C.: About the emissions of alternative jet fuels. CEAS Aeronaut. J. **8**, 167 (2017). https://doi.org/10.1007/s13272-016-0230-3
59. Zschocke, A., Scheuermann, S., Ortner, J.: High biofuel blends in aviation (hbba). Final Report No. ENER/C2/2012/420-1, Deutsche Lufthansa AG & Wehrwissenschaftliches Institut für Werk-und Betriebsstoffe, Germany (2012)
60. Voigt, C., Kleine, J., Sauer, D., Moore, R.H., Bräuer, T., Clercq, P.L., Kaufmann, S., Scheibe, M., Jurkat-Witschas, T., Aigner, M., Bauder, U., Boose, Y., Borrmann, S., Crosbie, E., Diskin, G.S., DiGangi, J., Hahn, V., Heckl, C., Huber, F., Nowak, J.B., Rapp, M., Rauch, B., Robinson, C., Schripp, T., Shook, M., Winstead, E., Ziemba, L., Schlager, H., Anderson, B.E.: Cleaner burning aviation fuels can reduce contrail cloudiness. Commun. Earth Environ. **2**, 114 (2021). https://doi.org/10.1038/s43247-021-00174-y
61. Burkhardt, U., Bock, L., Bier, A.: Mitigating the contrail cirrus climate impact by reducing aircraft soot number emissions. Clim. Atmos. Sci. **1**, 37 (2018). https://doi.org/10.1038/s41612-018-0046-4
62. Bock, L.: Modelling of contrail cirrus: Microphysical and optical characteristics [modellierung von kondensstreifenzirren: Mikrophysikalische und optische eigenschaften]. Ph.D. thesis, Ludwig–Maximilians-Universität München, Munich, Germany (2014)
63. Lee, D.S., Fahey, D.W., Skowron, A., Allen, M.R., Burkhardt, U., Chen, Q., Doherty, S.J., Freeman, S., Forster, P.M., Fuglestvedt, J., Gettelman, A., De León, R.R., Lim, L.L., Lund, M.T., Millar, R.J., Owen, B., Penner, J.E., Pitari, G., Prather, M.J., Sausen, R., Wilcox, L.J.: The contribution of global aviation to anthropogenic climate forcing for 2000 to 2018. Atmos. Environ. **244**, 117834 (2021). https://doi.org/10.1016/j.atmosenv.2020.117834
64. Marek, C.J., Smith, T.D., Kundu, K.: Low emission hydrogen combustors for gas turbines using lean direct injection, in Proc 41st AIAA/ASME/SAE/ASEE Joint Propulsion Conference and Exhibit (AIAA Meeting Paper, "Tucson, Arizona, United States", 2005)
65. Grewe, V., Bock, L., Burkhardt, U., Dahlmann, K., Gierens, K., Hüttenhofer, L., Unterstrasser, S., Rao, A.G., Bhat, A., Yin, F., Reichel, T.G., Paschereit, O., Levy, Y.: Assessing the climate impact of the AHEAD multi-fuel blended wing body. Meteorol. Z. **26**(6), 711 (2017). https://doi.org/10.1127/0941-2948/2005/0057
66. Ponater, M., Pechtl, S., Sausen, R., Schumann, U., Hüttig, G.: Potential of the cryoplane technology to reduce aircraft climate impact: a state-of-the-art assessment. Atmos. Environ. **40**(36), 6928 (2006). https://doi.org/10.1016/j.atmosenv.2006.06.036
67. Marquardt, S., Ponater, M., Ström, L., Gierens, K.: An upgraded estimate of the radiative forcing of cryoplane contrails. Meteorol. Z. **14**(4), 573 (2005). https://doi.org/10.1127/0941-2948/2005/0057
68. Air Transport Association of America: Standard method of estimating comparative direct operating costs of turbine powered transport airplanes. Tech. rep., The Association, Washington D.C., United States (1967)
69. Liebeck, R.H., Andrastek, D.A., Chau, J., Girvin, R., Lyon, R., Rawdon, B.K., Scott, P.W., Wright, R.A.: Advanced subsonic airplane design & economic studies. Tech. Rep. NASA CR–195443, McDonnell Douglas Corporation, Long Beach, California, United States (1995)
70. Association of European Airlines: Long range aircraft—AEA requirements (1989). G(T) 5655
71. Association of European Airlines: Short-medium range aircraft—AEA requirements (1989). G(T) 5656
72. Thorbeck, J., Scholz, D.: DOC-assessment method (2013). [Presentation] 3rd Symposium on Collaboration in Aircraft Design, Linköping, Sweden. https://www.fzt.haw-hamburg.de/pers/Scholz/Aero/TU-Berlin_DOC-Method_with_remarks_13-09-19.pdf. Accessed 22 July 2020
73. Pohya, A.A., Wicke, K., Hartmann, J.: Comparison of direct operating cost and life cycle cost-benefit methods in aircraft technology assessment, in Proc 2018 AIAA Aerospace Sciences Meeting. AIAA Scitech Forum, Kissimmee (2018)
74. Schnieder, H.: Methode zur Bewertung von Projekten und Technologien im zivilen Flugzeugbau. Tech. rep., Daimler-Benz Aerospace Airbus GmbH, Garching, Germany (1999). DGLR-Workshop, TU Munich
75. Ploetner, K.O., Schmidt, M., Baranowski, D., Isikveren, A.T., Hornung, M.: Operating cost estimation for electric-powered transport aircraft, in Proc 2013 Aviation Technology, Integration, and Operations Conference (AIAA Aviation Forum, Los

Angeles, California, United States, 2013). https://doi.org/10.2514/6.2013-4281
76. International Air Transport Association: IATA 2007 Report on Alternative Fuels. Tech. rep, International Air Transport Association (2007)
77. de Jong, S.A.: Green horizons: On the production costs, climate impact and future supply of renewable jet fuels. Ph.D. thesis, Utrecht University, Utrecht, The Netherlands (2018)
78. Bann, S.J., Malina, R., Staples, M.D., Suresh, P., Pearlson, M., Tyner, W.E., Hileman, J.I., Barrett, S.: The costs of production of alternative jet fuel: a harmonized stochastic assessment. Biores. Technol. **227**, 179 (2017)
79. Ram, M., Bogdanov, D., Aghahosseini, A., Gulagi, A., Oyewo, A.S., Child, M., Caldera, U., Sadovskaia, K., Farfan, J., Barbosa, L.S.N.S., Fasihi, M., Khalili, S., Dalheimer, B., Gruber, G., Traber, T., De Caluwe, F., Fell, H.J., Breyer, C.: Global energy system based on 100% renewable energy—power, heat, transport and desalination sectors. Tech. rep., Lappeenranta University of Technology and Energy Watch Group, Lappeenranta, Finland and Berlin, Germany (2019)
80. Graham, P., Reedman, L., Rodriguez, L., Raison, J., Braid, A., Haritos, V., Brinsmead, T., Hayward, J., Taylor, J., O'Connell, D.: Sustainable aviation fuels road map: data assumptions and modelling. Tech. rep, CSIRO (2011)
81. Pavlenko, N., Searle, S., Christensen, A.: The cost of supporting alternative jet fuels in the european union (2019). Working Paper, The International Council on Clean Transportation
82. Rojas, D., Crone, K., Löchle, S., Sigmund, S.: Powerfuels in aviation. Tech. Rep. Global Alliance Powerfuels, Deutsche Energie-Agentur GmbH (dena), Berlin, Germany (2019)
83. Brewer, G.D., Morris, R.E., Lange, R.H., Moore, J.W.: Volume II final report: Study of the application of hydrogen fuel to long-range subsonic transport aircraft. Tech. Rep. NASA CR–132559, Lockheed-California Company and Lockheed-Georgia Company, Hampton, Virginia, United States (1975)
84. Seeckt, K., Scholz, D.: Jet versus prop, hydrogen versus kerosene for a regional freighter aircraft, in Proc 58th Deutscher Luft- und Raumfahrtkongress. Deutsche Gesellschaft für Luft-und Raumfahrt, DGLR, Aachen (2009)
85. Seeckt, K.: Conceptual design and investigation of hydrogen-fueled regional freighter aircraft. Master's thesis, KTH Royal Institute of Technology, Stockholm, Sweden (2010)
86. Silberhorn, D., Hartmann, J., Dzikus, N.M., Atanasov, G., Zill, T., Brand, U., Trillos, J.C.G., Oswald, M., Vogt, T., Wilken, D., Grimme, W.: The air-vehicle as a complex system of air transport energy systems, in Proc AIAA AVIATION 2020 FORUM. AIAA Aviation Forum, Virtual Event (2020)
87. Mangold, J.: Economical assessment of hydrogen short-range aircraft with the focus on the turnaround procedure. Master's thesis, University of Stuttgart, Stuttgart, Germany (2021)
88. Fusaro, R., Viola, N., Ferretto, D., Vercella, V., Villace, V.F., Steelant, J.: Life cycle cost estimation for high-speed transportation systems. CEAS Space J. **12**, 213 (2020). https://doi.org/10.1007/s12567-019-00291-7
89. International Energy Agency: The future of hydrogen: Seizing today's opportunities. Tech. rep, International Energy Agency (2019)
90. Vercella, V., Ferretto, D., Fusaro, R., Viola, N., Villace, V.F., Steelant, J.: Towards future lh2 productive scenarios: Economic assessment and environmental effects on hypersonic transportation systems, in Proc HiSST: International Conference on High-Speed Vehicle Science Technology (Council of European Aerospace Societies (CEAS), Moscow, Russia, 2018)
91. Fusaro, R., Vercella, V., Ferretto, D., Viola, N., Steelant, J.: Economic and environmental sustainability of liquid hydrogen fuel for hypersonic transportation systems. CEAS Space J. **12**, 441 (2020). https://doi.org/10.1007/s12567-020-00311-x
92. Glenk, G., Reichelstein, S.: Economics of converting renewable power to hydrogen. Nat. Energy **4**, 216 (2019). https://doi.org/10.1038/s41560-019-0326-1
93. Creti, A., Kotelnikova, A., Meunier, G., Ponssard, J.: Research report: A cost benefit analysis of fuel cell electric vehicles (2015)
94. Christensen, A.: Assessment of hydrogen production costs from electrolysis: United states and europe (2020)
95. Commission, European: Communication from the commission to the european parliament, the council, the european economic and social committee and the committee of the regions. Tech. rep, European Commission, Brussels, Belgium (2020)
96. van den Bulk, J.: A cost- and benefit analysis of combustion cars, electric cars and hydrogen cars in the netherlands. Master's thesis, Wageningen University, Wageningen, The Netherlands (2009)
97. Brewer, G.D.: LH2 airport requirements study. Tech. Rep. NASA CR–2700, Lockheed-California Company, Burbank, California, United States (1976)
98. Torenbeek, E.: Advanced aircraft design. Wiley, Chichester (2013)
99. Lee, M., Li, L.K.B., Song, W.: Analysis of direct operating cost of wide-body passenger aircraft: A parametric study based on hong kong. Chin. J. Aeronaut. **32**(5), 1222 (2019). https://doi.org/10.1016/j.cja.2019.03.011
100. U.S. Energy Information Administration: Annual energy outlook 2022. Tech. rep., U.S. Energy Information Administration, Washington, DC, United States (2022). https://www.eia.gov/outlooks/aeo/pdf/AEO2022_Narrative.pdf. Accessed 20 June 2022
101. Bundesamt, S.: Erzeugerpreisindex für kerosin (flugturbinenkraftstoff aus leuchtöl) in deutschland in den jahren 2009 bis 2021 (2022). https://de.statista.com/statistik/daten/studie/505203/umfrage/preisentwicklung-kerosin-in-deutschland/. Accessed 20 June 2022
102. Reshotko, E.: Drag reduction by cooling in hydrogen-fueled aircraft. J. Aircr. **16**(9), 584 (1979)
103. Corchero, G., Montañés, J.L.: An approach to the use of hydrogen for commercial aircraft engines. Proceedings of the Institution of Mechanical Engineers, Part G: Journal of Aerospace Engineering **219**(1), 35 (2005). https://doi.org/10.1243/095441005X9139
104. Jackson, A.J.B.: Optimisation of aero and industrial gas turbine design for the environment. Ph.D. thesis, Cranfield University, Cranfield, United Kingdom (2009)
105. Stiller, C., Schmidt, P.: Airport liquid hydrogen infrastructure for aircraft auxiliary power units, in Proc 18th World Hydrogen Energy Conference 2010. Verlag Jülich, Essen, Germany, Forschungszentrum Jülich GmbH Zentralbibliothek (2010)